ChemCatChem

How could the physical properties of poly(vinyl alcohol) influence enzymatic activity? Detailed study on nanofibrous enzyme catalysts

--Manuscript Draft--

Manuscript Number:	cctc.202400562
Article Type:	Research Article
Corresponding Author:	Diana Balogh-Weiser, PhD Budapest University of Technology and Economics Budapest, HUNGARY
Corresponding Author E-Mail:	balogh.weiser.diana@vbk.bme.hu
Order of Authors (with Contributor Roles):	Gergő Dániel Tóth (Data curation: Lead; Formal analysis: Lead; Investigation: Lead; Methodology: Equal; Writing – original draft: Lead)
	Zsófia Molnár, PhD (Conceptualization: Supporting; Formal analysis: Supporting; Investigation: Equal; Methodology: Supporting; Visualization: Supporting)
	Gábor Koplányi (Investigation: Supporting)
	Benjámin Gyarmati, PhD (Investigation: Supporting; Methodology: Supporting)
	András Szilágyi, PhD (Funding acquisition: Supporting; Methodology: Supporting; Writing – review & editing: Supporting)
	Gábor Katona, PhD (Formal analysis: Equal; Investigation: Supporting; Visualization: Supporting)
	Alfréd Menyhárd, PhD (Formal analysis: Supporting; Investigation: Supporting)
	László Poppe, DSc (Methodology: Supporting; Writing – review & editing: Supporting)
	Béla Pukánszky, DSc (Supervision: Supporting; Writing – review & editing: Supporting)
	Diana Balogh-Weiser, PhD (Funding acquisition: Lead; Methodology: Equal; Resources: Lead; Supervision: Lead; Writing – review & editing: Lead)
Keywords:	biocatalysis, poly(vinyl alcohol), nanofibers enzyme immobilization
Manuscript Classifications:	Biocatalysis
Suggested Reviewers:	Lucia Gardossi Professor, University of Trieste gardossi@units.it Expert in biocatalysis and enzyme immobilization.
	Jairo Oliveira Professor, Federal University of Espirito Santo jairo.oliveira@ufes.br Expert in nanomaterials chemistry and enzyme-nanocarrier interactions.
	Rudi Fasan Professor, University of Rochester fasan@chem.rochester.edu Expert in synthetic biocatalysis.
	Francesca Paradisi University of Bern francesca.paradisi@unibe.ch Expert in biocatalysis and the development of enzyme immobilization process and carrier design.
Opposed Reviewers:	

Abstract:	The immobilization of enzyme catalysts within polymer nanofibers is increasingly influential across scientific and industrial sectors. Utilizing electrospinning technique to entrap enzymes within nanofibers (providing nanofibrous enzyme catalysts, NEC) offers promising avenues for technological advancement. While numerous instances of poly(vinyl alcohol) (PVA)-based nanofibrous biocatalysts have been documented, a comprehensive investigation to thoroughly characterize the process and effect of PVA on catalytic activity is notably lacking. This study systematically investigates the effect of PVA properties, such as molecular weight, degree of hydrolysis, and polymer concentration, on the structure of PVA nanofibers and on the biocatalytic properties of a lipase from Burkholderia cepacia (BcL) entrapped into PVA nanofibers. The PVA-enzyme interactions were studied using viscometry, scanning electron microscopy, Raman mapping, differential scanning calorimetry and computational docking simulations. The natural back-and-forth catalytic process (stereoselective hydrolysis and transesterification) of the lipase was used to evaluate the enzyme activity. Results showed that the molecular weight and degree of hydrolysis of PVA have significant effect on the biocatalytic activity of nanofibrous enzyme catalysts (almost fully hydrolyzed PVA with 61 kDa molecular weight provided tenfold increase in enzymatic activity of BcL compared to its native form).
Author Comments:	Official cover letter had been uploaded to the submission portal.
Section/Category:	
Additional Information:	
Question	**Response**
Do you agree to comply with the legal and ethical responsibilities outlined in the journal's Notice to Authors?	Yes
Has a previous version of this manuscript been submitted to this journal?	No
Is this manuscript, or part of it, currently under consideration elsewhere?	No
Is this manuscript, or part of it, published, posted, or in press? This includes content posted on preprint servers (preprint guidelines) or published as part of a thesis.	No
Please provide us with information about the history of your manuscript, including previous submissions, transfers, or prior versions:	This is the first time to publish this research, there no other submission initiated.
Do you or any of your co-authors have a conflict of interest to declare?	No
Does the research described in this manuscript include animal experiments?	No
Does the research described in this manuscript include human research participants (including for experiments with sensors or wearable technologies) or tissue samples from human subjects (including blood or sweat)?	No

WILEY VCH

CONCEPT

How could the physical properties of poly(vinyl alcohol) influence enzymatic activity? Detailed study on nanofibrous enzyme catalysts

Gergő Dániel Tóth[a,b], Zsófia Molnár[c], Gábor Koplányi[c], Benjámin Gyarmati[a], András Szilágyi[a], Gábor Katona[d], Alfréd Menyhárd[a], László Poppe[c], Béla Pukánszky[a,e], Diána Balogh-Weiser[a,b,c]*

[a] G. D. Tóth, Dr. B. Gyarmati, Dr. A. Szilágyi, Dr. A. Menyhárd, Prof. Dr. B. Pukánszky, Dr. D. Balogh-Weiser
Department of Physical Chemistry and Materials Science, Faculty of Chemical Technology and Biotechnology
Budapest University of Technology and Economics
Műegyetem rkp. 3., H-1111 Budapest, Hungary
E-mail: balogh.weiser.diana@vbk.bme.hu

[b] G.D. Tóth, Dr. D. Balogh-Weiser
Spinsplit Llc., Szőllőskert u.0182/135, H-2220 Vecsés, Hungary

[c] Dr. Zs. Molnár, G. Koplányi, Prof. Dr. L. Poppe, Dr. D. Balogh-Weiser
Department of Organic Chemistry and Technology, Faculty of Chemical Technology and Biotechnology
Budapest University of Technology and Economics
Műegyetem rkp. 3., H-1111 Budapest, Hungary

[d] Dr. G. Katona
Institute of Pharmaceutical Technology and Regulatory Affairs Faculty of Pharmacy,
University of Szeged
Eötvös u. 6., H-6720 Szeged, Hungary

[e] Prof. Dr. B. Pukánszky
Institute of Materials and Environmental Chemistry,
Research Centre for Natural Sciences
H-1519, Budapest, Hungary

Abstract: The immobilization of enzyme catalysts within polymer nanofibers is increasingly influential across scientific and industrial sectors. Utilizing electrospinning technique to entrap enzymes within nanofibers (providing nanofibrous enzyme catalysts, NEC) offers promising avenues for technological advancement. While numerous instances of poly(vinyl alcohol) (PVA)-based nanofibrous biocatalysts have been documented, a comprehensive investigation to thoroughly characterize the process and effect of PVA on catalytic activity is notably lacking. This study systematically investigates the effect of PVA properties, such as molecular weight, degree of hydrolysis, and polymer concentration, on the structure of PVA nanofibers and on the biocatalytic properties of a lipase from *Burkholderia cepacia* (*Bc*L) entrapped into PVA nanofibers. The PVA-enzyme interactions were studied using viscometry, scanning electron microscopy, Raman mapping, differential scanning calorimetry and computational docking simulations. The natural back-and-forth catalytic process (stereoselective hydrolysis and transesterification) of the lipase was used to evaluate the enzyme activity. Results showed that the molecular weight and degree of hydrolysis of PVA have significant effect on the biocatalytic activity of nanofibrous enzyme catalysts (almost fully hydrolyzed PVA with 61 kDa molecular weight provided tenfold increase in enzymatic activity of *Bc*L compared to its native form).

1. Introduction

Enzymes play indispensable roles in catalyzing vital life-sustaining processes to facilitate the sufficient reaction rates under physiological conditions.[1] However, the utilization of pure enzymes is often economically impractical[2], especially considering the requisite cofactors which can also be costly.[3] Traditional liquid-liquid separation techniques typically fail to recover efficiently both enzymes and cofactors employed in homogeneous catalysis.[4] Furthermore, the inherent stability of biocatalysts is generally lower compared to that of conventional synthetic catalysts, with optimal performance typically observed under mild physiological conditions.[5, 6]

To overcome these challenges, various enzyme immobilization strategies have been developed, aiming to retain or enhance the catalytic activity, specificity, and selectivity.[7–10] Lipases, a subclass of enzymes catalyzing ester bond hydrolysis or synthesis, present particular interest due to their dual activity in aqueous and organic media. In aqueous environments, lipases predominantly exhibit hydrolytic activity, while in organic solvents, their synthetic activity becomes prominent. Given their versatile nature, lipases find applications across diverse industries including pharmaceuticals, food processing, detergents, leather production, and oil refining.[11–14]

Polymers displaying specific attributes such as inertness, as well as physical and chemical stability are predominantly used as carriers for the immobilization of enzymes. These requirements can be met by polymers of both natural and synthetic origins.[15] The benefit of using synthetic polymers as enzyme carriers is that

the monomers that make up the polymer chain can be chosen to ensure specific binding groups for enzyme immobilization via physical or chemical interactions. The type and repeating units of monomers determine the chemical structure and properties of the polymers.[16–19] Biopolymers, such as water-insoluble polysaccharides like cellulose[20], chitin[21], agarose[22], carrageenans[23], and chitosan[24], have all been utilized as supports for immobilizing enzymes. Furthermore, cross-links can be formed to strengthen the structure and boost mechanical and thermal resistance.[25] From appropriately selected polymers, a range of techniques is available to produce nano-scale supports suitable for enzyme immobilization. These techniques include electrohydrodynamic processing methods such as electrospinning[26], electrospraying[27], in addition, vapor condensation[28], solvent evaporation[29], nanoprecipitation[30], emulsification on a solvent diffusion[31], and reverse salting out[32]. The techniques listed above can produce various supports with different structures and shapes. These include quasi-zero-dimensional spheroids[33], quasi-one-dimensional nanorods[34] or nanofibers, and quasi-two-dimensional planar structures, like nanodiscs.[35]

One of the most promising techniques for producing nanoscale supports nowadays is electrostatic fiber formation (electrospinning). Solid fibrous polymer structures with a huge specific surface area and submicron diameter can be produced by its use.[26] These structures can immobilize (bio)catalysts[36], form special drug formulations[37], preserve biological samples[38], form synthetic membrane structures suitable for filtration[39], and even produce textiles for clothing.[40] During the spinning process, when a sufficiently high voltage is applied to a polymer droplet, electrostatic repulsion occurs between the equally charged polymer particles. If the repulsive force between the charged particles exceeds the magnitude of the cohesive forces holding the droplet together, a fluid flow will burst from the surface of the elongated droplet (so-called *Taylor cone*) at a critical point, and solid nanosized fibrous product can be collected on the collector plate.[41] Nanofibers can be used for either surface immobilization or entrapment of enzymes or cells.[42, 43] The main advantages of the entrapment method are that the immobilization process can be carried out in a remarkably short time and the polymer matrix formed during immobilization surrounds the entrapped proteins, thus providing a high degree of protection against their environment.

Poly(vinyl alcohol) (PVA) is commonly used in the production of papers and adhesives.[44, 45] Remarkably, PVA is one of the few polymers with outstanding biocompatibility and safety approved by the FDA for clinical usage in humans.[46] PVA is made by polymerizing vinyl acetate and then catalyzing the hydrolysis of the resultant poly(vinyl acetate). The main physical characteristics of the poly(vinyl alcohol) thus obtained are the average molecular weight and the number of residual acetyl groups (degree of hydrolysis).[47] Although there are articles in the literature on the electrostatic fiber formation of PVA, no research has been done to investigate in depth the effect of PVA properties such as molecular weight and degree of hydrolysis on electrospinning. Furthermore, a common flaw in studies about using PVA for creating supports for enzyme immobilization (including electrostatic fiber formation) is that they do not specify what kind of poly(vinyl alcohol) is used in the research, as presented in Figure 1.

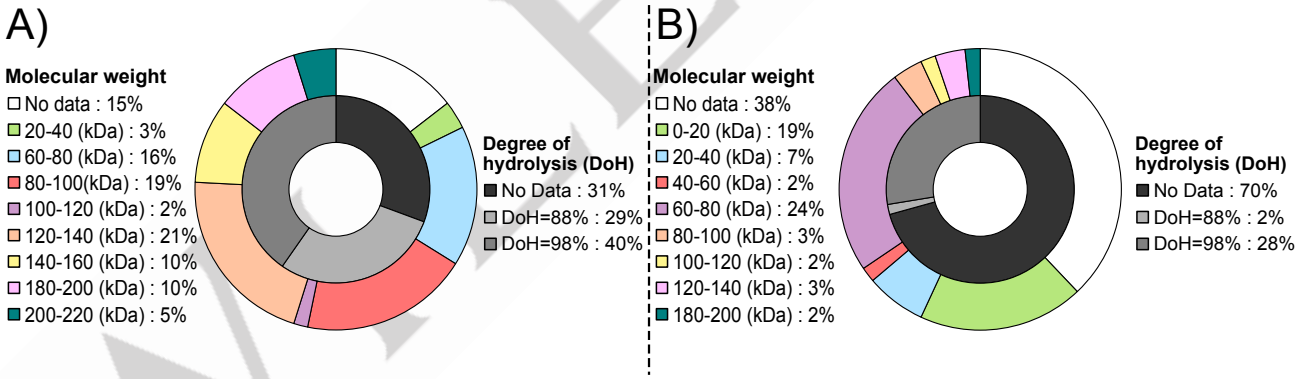

Figure 1. Distribution molecular weights and degrees of hydrolysis of poly(vinyl alcohol) typically used for the preparation of supports for enzyme immobilization, based on literature search has been conducted by utilizing Google Scholar with the search terms 'PVA AND enzyme immobilization' and 'PVA AND enzyme immobilization AND electrospun nanofibers', limiting results from 1994 to the present (the past 30 years). Subsequently, the first 50 most relevant articles for the first search phrase and the first 48 most relevant articles for the second search phrase were accessed. Supports with **A)** fibrous and **B)** other structures were grouped separately.[11–14, 48–141]

Figure 1 illustrates that a broad molecular weight range of PVA is utilized for the synthesis of enzyme supports. Based on the data in the figure, we can infer that PVA of molecular weights of 120–140 kDa is most used for enzyme supports with fibrous structure. Conversely, non-fibrous enzyme supports tend to favor PVA of 60-80 kDa molecular weights. Across both categories, fully hydrolyzed PVA appears to be the preferred choice. However, it is important to note that these selections often reflect ad hoc decisions, rather than systematic preferences.

The electrostatic fiber forming ability of PVA is well known. Water solubility is a great advantage of PVA because its electrospinning can be achieved from aqueous precursor solutions. Recent studies report on successful entrapment of cellulase[48], lipase[49], transferase[50], α-amylase[51], and protease[52] enzymes in PVA nanofibers, among others.

The aim of this study is to thoroughly investigate the electrostatic fiber-forming ability of aqueous precursor solutions containing various concentrations of commercially available PVA with different molecular weights and degrees of hydrolysis to form nanofibrous

polymer matrices suitable for enzyme immobilization. Although there exist numerous examples about the application of PVA nanofibers for enzyme immobilization, comprehensive studies about the effect of PVA properties on the process is still missing. In this study, the effect of PVA properties was systematically investigated on fiber formation conditions (precursor composition, voltage, collector-emitter distance, feed rate), on the morphology of the produced nanofiber systems, on the rheological properties of the precursor solutions, and on the apparent activity of the model enzyme (*Burkholderia cepacia* lipase, *Bc*L) in the forming nanobiocatalysts involving experimental and computational studies. The *Bc*L entrapped in PVA nanofibers were investigated in detail. Besides the exploration of PVA-enzyme interactions, the aim of the work is to find the optimal nanofibrous PVA carrier system to produce effective Nanofibrous Enzyme Catalysts (NEC) (Figure 2).

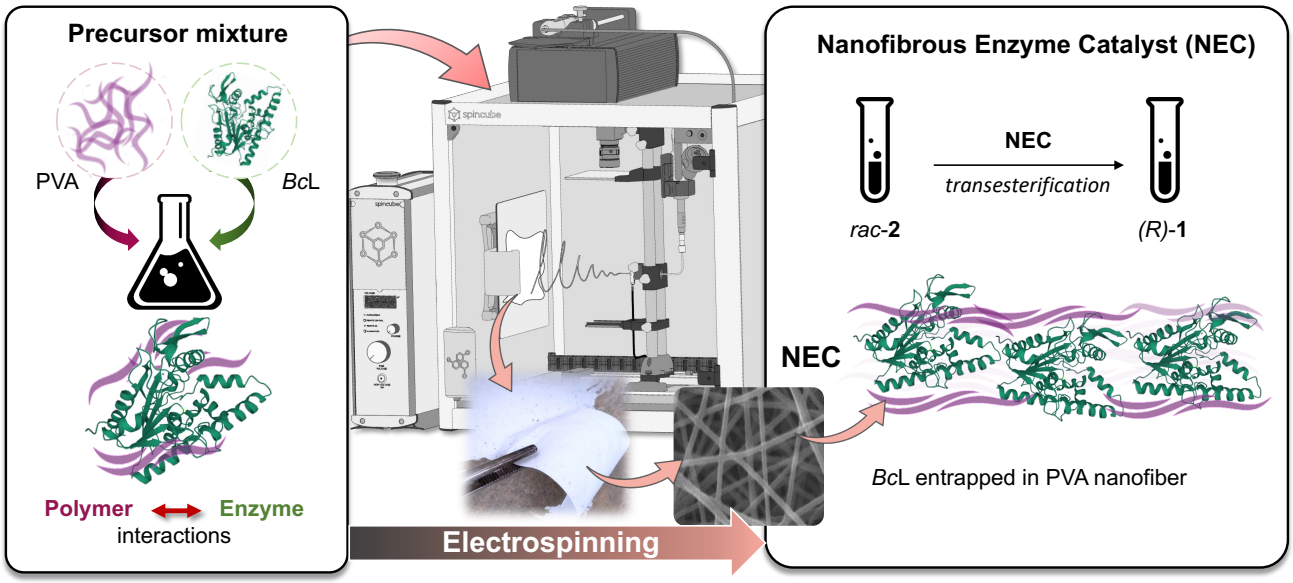

Figure 2. The production of Nanofibrous Enzyme Catalyst (NEC) from aqueous precursor mixture of poly(vinyl alcohol) (PVA) and *Burkholderia cepacia* lipase (*Bc*L) by the electrospinning technique and transesterification of racemic 2-octanol (*rac*-**2**) to (*R*)-2-octylacteate ((*R*)-**1**) catalyzed by NEC.[142]

2. Materials and Methods

2.1. Materials

Lipase from *Burkholderia (Pseudomonas) cepacia* (Amano Lipase PS crude enzyme powder, 534641, *Bc*L), racemic 2-octanol (*rac*-**2**), poly(vinyl alcohol) (PVA) with DoH 88%: Mowiol® 3-88 (*MW*=24kDa), 4-88 (*MW*=31kDa), 8-88 (*MW*=67kDa), 18-88 (*MW*=130kDa), 40-88 (*MW*=205kDa) and with DoH 98%: 4-98 (*MW*=27kDa), 6-98 (*MW*=47kDa), 10-98 *MW*=61kDa), 20-98 (*MW*=125kDa), 56-98 (*MW*=195kDa), vinyl acetate (VA), *tert*-butyl methyl ether (MTBE), *n*-hexane, ethanol, 2-propanol (IPA), hydrochloric acid, sodium hydroxide, sodium phosphate monobasic were purchased from Merck (Saint Louis, MO, USA). In all cases, the water was purified (ρ > 18.2 MΩ cm) by a Millipore Milli Q water purification system (Bradford, MA, USA). Substrate *rac*-2-octyl acetate (*rac*-**1**) was synthetized as follows. In a 200 mL Erlenmeyer flask, 60 mL of *n*-hexane and 30 mL of MTBE were added to 2 g of Immozyme CaLA-T2-150 (ChiralVision, Den Hoorn, Netherlands). Then 5 mL of *rac*-**2** and 10 mL of VA were added to the mixture. The reaction was stirred in a 40 °C water bath. After 6 h CaLA-T2-150 was filtered through a glass filter (G4) and washed with n-hexane (three times 50 mL). The filtrate was evaporated on a rotary vacuum evaporator. The structure of product *rac*-**1** was determined with nuclear magnetic resonance spectroscopy (NMR); 1H NMR (500 MHz, DMSO-d6) δ 4.82–4.73 (m, 1H), 1.98 (s, 2H), 1.52–1.44 (m, 1H), 1.33–1.18 (m, 6H), 1.15 (d, J = 6.3 Hz, 2H), 0.86 (t, J = 6.7 Hz, 2H) with a Bruker Avance 500 MHz multinuclear NMR spectrometer.

2.2. Measurement of the catalytic activity of native *Bc*L lipase in presence of different PVA polymers

The lipase activity assay in aqueous media was performed as follows. Solutions of 4 mg mL^{-1} in sodium phosphate buffer (50 mM, pH = 7.5) were prepared from all type of PVAs (see Section 2.1) and a PVA-free solution was also prepared and tested as reference. To 500 µL of this solution, 500 µL of lipase solution (12 mg mL^{-1}; in phosphate buffer: 50 mM, pH = 7.5) and 100 µL of isopropanol cosolvent were added, and finally 25 µL of *rac*-**1** was added. The resulting reaction mixture was shaken for 2 h at 30 °C in a shaker incubator at 450 rpm (Heidolph, Titramax 100). After that, 50 µL of the mixture was sampled, diluted with 450 µL of ethanol and analyzed using a chiral gas chromatograph (GC) [Agilent 4890D] with Hydrodex-β-6-TBDM (25 m×0.25 mm×0.25 mm film) stationary phase. The time of retention (t_R) of compounds were the following: (*R*)-**2**+(*S*)-**2**: 10.5 min, (*S*)-**1**: 11.0 min, (*R*)-**1**: 13.7 min. The parameters determined in the evaluation of the chromatograms are summarized in Section 2.9.

2.3. Production of PVA nanofibers

The precursor solutions used for fiber formation were obtained by dissolving the appropriate PVA (see Section 2.1) in Milli Q water. PVA solutions of 6, 8, 10, 12, 14 and 16 wt% were performed in a 50 °C water bath using a magnetic stirrer. The electrospinning experiments were performed using a SpinCube (Spinsplit, Budapest, Hungary) electrostatic fiber-forming device. The precursor solutions were delivered from a single use sterile syringe (3 mL) through a G18 needle (emitter) connected by a PTFE tube (1/16 OD, dead volume: 250 µL) using a syringe pump. The fibrous product was collected on an aluminum foil attached to the collector. The experiments were performed at room temperature. The voltage (typically in the range $12 < U < 14$ kV), dosing rate ($0.01 < V < 0.03$ mL min^{-1}) and emitter-collector distance ($12 < l < 16$ cm) were systematically tuned to achieve fiber formation.

2.4. Production of NEC (*Bc*L entrapped in PVA nanofibers)

To immobilize the *Bc*L enzyme, an amount of enzyme solution (100 mg mL^{-1} in phosphate buffer 50 mM; pH= 7.5) was added to the precursor solutions prepared in Section 2.3 so that the fibrous catalyst prepared from the resulting nanofibrous mat contained 5 wt% of the lipase. The resulting system was thoroughly homogenized using a vortex, and then the fiber formation experiment was performed as described in Chapter 2.3.

2.5. Rheological characterization

The viscosity of the lipase-free and lipase-containing precursor PVA mixtures was determined by a Physica MCR 301 rotational rheometer (Anton Paar, Graz, Austria). A probe with a cone–plate geometry (with a diameter of 25 mm and cone angle of 1°) was used for the tests. The measuring chamber of the instrument was thermostated at 25.0 °C for each sample, and the interval of shear rate was 1–631 s^{-1}. Every experiment was performed triplicate.

2.6. Morphological characterization

Morphology of nanofiber matrices was studied by a JSM JEOL-5500LV (JEOL, Tokyo, Japan) SEM-EDS scanning electron microscope (SEM). The samples were placed on copper grids. To ensure adequate surface conductivity, the samples were coated with gold in a few atomic layers of thickness by a nebulizer (Polaron sc760 mini sputter coater, Thermo VG Microtech, Waltham, MA, USA) using argon-plasma, at 10 mA for 180 s. The images were taken in the high vacuum mode of the SEM and were processed using a digital image evaluation software (ImageJ 1.53r, U.S. National Institutes of Health) to determine the average fiber diameter and standard deviation of the nanofibrous samples (n = 100).

2.7. Characterization of *Bc*L entrapped In PVA Nanofibers Via Raman Mapping

Raman mapping of nanofibers was performed by a Thermo Fisher DXR dispersive Raman instrument (Thermo Fisher Scientific Inc., Waltham, MA, USA) equipped with a CCD camera and a diode laser operating at the wavelength of 780 nm. For sample preparation, a glass slide was covered with aluminum foil containing electrospun nanofibers. A Raman chemical map was obtained from a 100 × 100 µm surface of different nanofibers with a 1×1 µm spectral resolution while applying a laser power of 12 mW at a 50 µm slit aperture size. The spectrum of the chemical map was recorded with an exposure time of 2 s and acquisition time of 6 s, for a total of 32 scans per spectrum in the spectral range 3300–200 cm^{-1} with cosmic ray and fluorescence corrections. Each Raman map was normalized to eliminate the intensity deviation among the measured areas.

2.8. Catalytic activity measurement of NEC (*Bc*L entrapped in PVA nanofibers)

A solvent mixture (1.0 mL of a *n*-hexane:MTBE, 2:1, V:V), of *rac*-**2** (50 µL), and VA (100 µL) were added to 10.0 mg of the NEC (*Bc*L entrapped in PVA nanofibers) in a screw-capped glass vial (4 mL). The reaction mixture was shaken with an orbital shaker (at 450 rpm) at 30 °C. After 2, 4 and 24 h, 50 µL of the mixture was sampled, diluted with 450 µL of ethanol, and analyzed using gas chromatograph (GC) (Agilent 4890D) equipped with a Hydrodex-β-6-TBDM capillary column (25 m×0.25 mm×0.25 mm film) with a chiral stationary phase. The parameters determined in the evaluation of the chromatograms are summarized in Section 2.9.

2.9. Calculation of biocatalytic parameters

The following parameters for determining the biocatalytic activity were calculated from the chromatograms: conversion [(c; %) $c = n_P \times (n_S + n_P)^{-1} \times 100$], specific biocatalyst activity [(U_B; U g^{-1}) $U_B = n_s \times c \times (t \times m_B)^{-1}$], specific enzyme activity [(U_E, U g^{-1}) $U_E = n_s \times c \times (t \times m_E)^{-1}$], activity yield [($Y_A$; %) $Y_A = U_{E,native} \times U_{E,immobilized}^{-1} \times 100$], where n_P and n_S are the molar amounts of product (P) and substrate (S) [µmol], t is the time elapsed [min], m_B is the mass of the biocatalyst [g], m_E is the mass of the enzyme [g].

2.10. Calorimetric measurements

The calorimetric measurements were performed by a PerkinElmer DSC 8500 differential scanning calorimeter (PerkinElmer Inc., Waltham, Massachusetts, USA). The sample masses were between 3 and 5 mg and the samples were placed in hermetically sealed aluminum crucibles. High purity nitrogen was used as purge gas with a flow rate of 20 mL min^{-1}. The samples were conditioned at −20 °C for 2 min to establish stable starting condition, then the samples were heated up to 150 °C. Subsequently, the samples were held there for 2 min and cooled down to −20 °C, where they were conditioned for additional 2 min. Finally, the samples were reheated to 150 °C again. The heating

and cooling rates were 10 °C min^{-1} during all tests. T_g values were read from the first heating run.

2.11. Molecular docking

PVA oligomers of different degrees of hydrolysis (88 and 98 %) and monomer number (n=12; 15; 19) were used as polymer mimicking ligands. The structures of the PVA ligands were built using the Avogadro2.[143] Molecular docking was carried out on a personal computer using AutoDock Vina[144] via DockingPie[145], plugin with the open source PyMOL[146] plugin. For the receptors, two structures of *Bc*L were used, an *apo* structure displaying open lid (PDB ID: 2LIP) and an open lid structure complexed with hexylphosphonic acid (*R*)-2-methyl-3-phenylpropyl ester inhibitor (PDB ID: 1YS1). Receptors for ligand docking were prepared in the DockingPie module, the hexylphosphonic acid (*R*)-2-methyl-3-phenylpropyl ester inhibitor from 1YS1 and water were removed from both structures. Hydrogen atoms were added by the program. The grid box was centered (X = 15.9; Y = 1.1; Z = 20.0) and sized (spacing 5 Å, size 14; 15; 14 respectively) in a manner that the entire protein could fit in it to ensure that ligands would be able to dock on the surface and in the active site pocket as well. For every ligand-receptor combination, 10 poses were generated, the exhaustiveness and energy range were both set to 8.

To draw the correct conclusions about the behavior of PVA polymer chains and the possible interactions with *Bc*L, docking results were validated according to the following procedure: a plane was generated in PyMol[147] that passed through atoms Phe52/CZ, Leu293/CD2 and Phe119/CZ. The plane inserted this way covered the active site pocket of the enzyme. All docked ligands were manually analyzed whether their conformation could be interpreted as it were a part of a larger polymer chain. If both ends of the docked ligand were outside the plane, they were considered as polymer mimicking ligands and were used for further evaluation. If one or both ends were in-the-pocket side of the plane, such poses were considered as non-polymer-mimicking artefacts and were not used in further analysis. Results were analyzed visually in PyMOL, affinity energy results were plotted in R.[148]

3. Results and discussion

A comprehensive set of experiments was performed to investigate the effect of PVA on nanofiber formation and enzyme immobilization. The commercially available PVAs used differ in their degree of hydrolysis (DoH, %). Partially hydrolyzed grades have a DoH of about 88 %, while fully hydrolyzed grades have a DoH of about 98 %.The PVAs also differ in their molecular weight (MW_{PVA}: 24, 31, 67, 130, 205 kDa of DoH 88 % and 27, 47, 61, 125 and 195 kDa of DoH 98 %) were selected for the precursor solutions at different concentrations (c_{PVA}: 6, 8, 10, 12, 14 and 16 wt%). In total, 60 different PVA precursor solutions were prepared (Figure 3), and lipase from *Burkholderia cepacia* (*Bc*L) was used as a model enzyme. Although some of the PVA-containing precursor solutions, used for enzyme immobilization by electrospinning, can be found in the literature (see Figure 1), they are isolated cases. Here, the systematic examination of PVA-enzyme systems is presented by rheological investigations, enzyme activity assays of precursor solutions, SEM and Raman microscopic mapping and enzyme activity measurements of nanofibers.

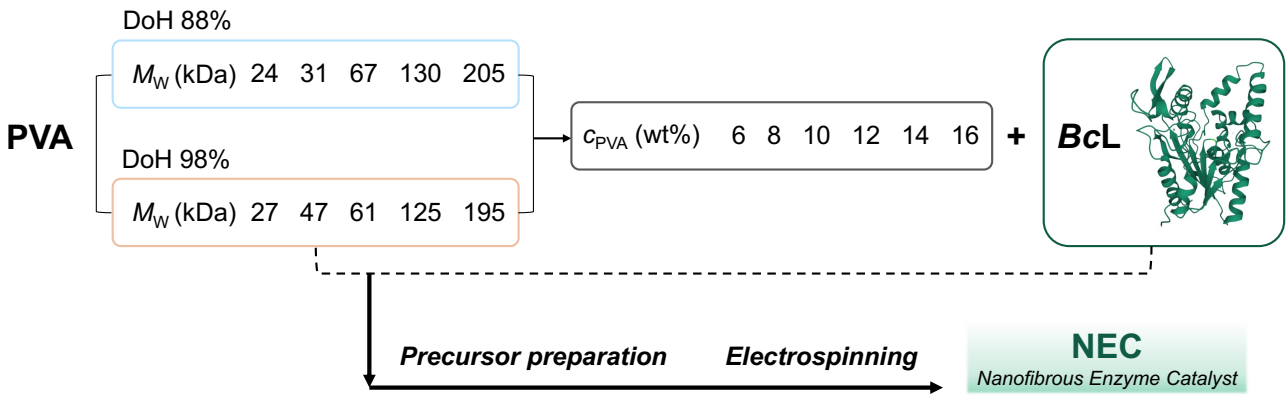

Figure 3. The experimental set of PVA-containing precursor solutions for the immobilization of *Bc*L in PVA nanofibers (NEC) using solvent electrospinning technique.

3.1. Effect of different PVA polymers on the activity of the native enzyme

Before investigating the activity of the immobilized enzymes, it was important to determine whether the presence of the PVA polymers used for the immobilization of the lipases affected their catalytic activity. In the case of hydrolytic enzyme catalysis (common among applications involving lipases), PVA matrices are also solubilized next to the protein. The presence of the dissolved polymer could possibly influence the catalytic reaction by the changes in the viscosity of the reaction media, or polymer chains could directly interact with enzyme molecules. Thus, it was necessary to verify that any changes observed in the apparent activity of the immobilized enzymes were indeed induced by the immobilization process and not simply by the presence of the polymer as an additive. To investigate the possible effect of PVA,

the lipase-catalyzed stereoselective hydrolysis of *rac*-**1** to (*R*)-octan-2-ol (according to Section 2.2) without PVA and in the presence of different PVAs (MW_{PVA}: 24, 31, 67, 130, 205 kDa of DoH 88 % and 27, 47, 61, 125 and 195 kDa of DoH 98 %) were carried out. To examine the influence of the polymers on the rheology of the reaction media, the viscosity using the same PVA content as that found in the dissolved NEC was investigated. Figure 4 shows the effect of different PVAs on the specific enzyme activity, U_E (Figure 4A), and viscosity (Figure 4B). In our statistical analysis of the measured activity and viscosity values, we used a single-factor Analysis of Variance (ANOVA) to find the significant differences among the data groups. The activity data met the requirements for equal variances (as confirmed by Levene's test), so no adjustments to the ANOVA calculation were needed. The results show that the PVA molecular weight has a substantial impact on the measured U_E (P<0.001; η^2=0.697). We then ran a standard post-hoc analysis to see how the sample groups differed from the reference point (native *Bc*L). For the viscosity data, we had to apply a Welch correction because the variances weren't equal according to the Levene's test. After the correction, our ANOVA test showed that the molecular weight of PVA significantly impacts the viscosity (P<0.001; η^2=0.869) as expected. We followed up with a Games-Howell post-hoc analysis to determine the differences of the sample groups from the reference (phosphate buffer). In both post-hoc tests Tukey correction was used for the calculation of P values, significant differences found compared to the reference measurements are shown in Figure 4. Statistical calculations were made with JASP.[149] In most cases, the presence of the polymer slightly reduced the lipase activity (U_E), but this decrease was not significant in the majority of the cases (Figure 4A). Figure 4B illustrates the absence of a clear correlation between the observed U_E values and the viscosity of the reaction media. Notably, the measured viscosity values exhibit minimal differences from one another, with their standard deviations consistently overlapping across all cases. This observation suggests that PVAs dissolved in low concentrations exert negligible influence on the viscosity of the reaction media. This inspection is supported by the results of the ANOVA calculation, revealing no significant deviation from the reference phosphate buffer (η = 0.91 ± 0.11 mPas; no dissolved PVA).

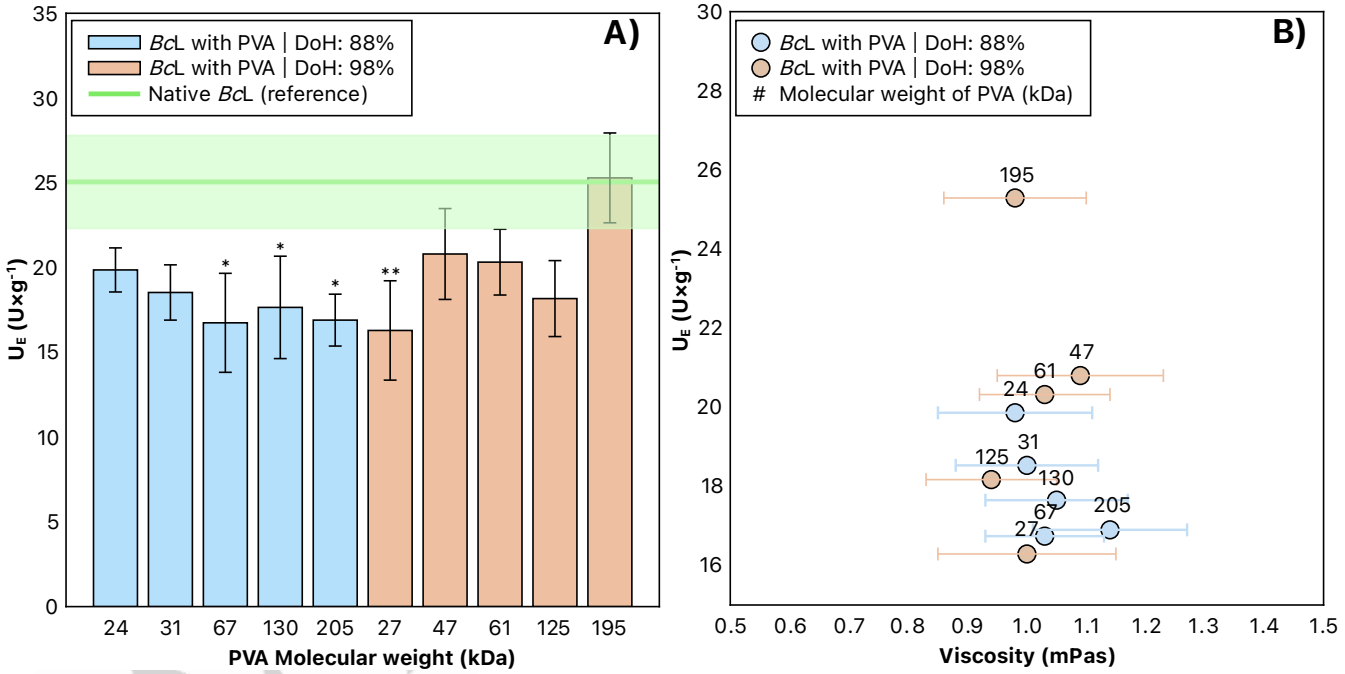

Figure 4. A) The effect of different PVAs with different molecular weights and degrees of hydrolysis (DoH) on the specific enzyme activity of, *Bc*L in the hydrolysis of *rac*-**1**. Test reactions were carried out in aqueous phosphate buffer (50 mM, pH = 7.5) at 30 °C under constant shaking. The specific enzyme activities (U_E, U×g^{-1}) were measured after 2 hours of reaction time. **B)** The influence of viscosity of PVAs with different molecular weights and DoH in aqueous phosphate buffer solutions (50 mM, pH = 7.5) was investigated through rotational viscometry analysis at 25 °C. The PVA concentration of the solutions tested was 2 mg×mL^{-1} in all cases. Dynamic viscosity values were calculated at 10 s^{-1} shear rate (γ). For each sample group significant differences found in the ANOVA post-hoc analysis compared to the reference measurements are denoted with asterisks (* p < 0.05, ** p < 0.01).

Viscosity stands as a pivotal parameter influencing the efficacy of the electrospinning process.[150] To determine the impact of the molecular weight and degree of hydrolysis of PVA on the viscosity of precursor solutions, and to pinpoint the viscosity threshold posing a technical constraint on the fiber-forming capacity of our electrospinning apparatus, viscosity measurements were conducted on both enzyme-free and enzyme-containing precursor solutions. Results presented in Figure 5 show that as the molecular weight of the polymer and the concentration of PVA grow, the viscosity of the solutions increases monotonously – caused by an increased degree of cohesion between the polymer molecules.[151] It is noteworthy that the viscosity of solutions containing PVAs hydrolyzed to varying extents, with similar molecular weights and concentrations, consistently exhibited higher values for fully hydrolyzed (DoH = 98%) PVA. The higher viscosity observed in fully hydrolyzed PVA aqueous solutions can be attributed to augmented intermolecular interactions among polymer molecules, as the increased number of free OH groups

enhance the statistical likelihood of the formation of both inter- and intra-chain hydrogen bonding.[152] A further consequence of the stronger interaction in the set of polymer molecules is that the dissolution of fully hydrolyzed PVA in water requires significantly more time and energy than the partially (88%) hydrolyzed PVA. By parallel examination of viscosity of the enzyme-containing and enzyme-free solutions, it can be concluded that the viscosity of the enzyme-containing solutions was always lower. As per the literature, a solution containing several polymeric macromolecules might have a viscosity that is either intermediate or greater than the solutions containing the individual components.[153] The side chains of amino acids in proteins include many reactive functional groups, which allow them to interact in a variety of ways with polymers in solution.[154] Thus, the type of polymer and its particular interactions with the protein might affect the conformation that the polymer adopts.[155] The drop in viscosity may indicate the development of a random coil shape around the protein, as globular structures are known to have significantly lower viscosities in solutions for both polymers and proteins.[154] It has previously been reported that such globular polymer-protein conjugates can indeed form.[156]

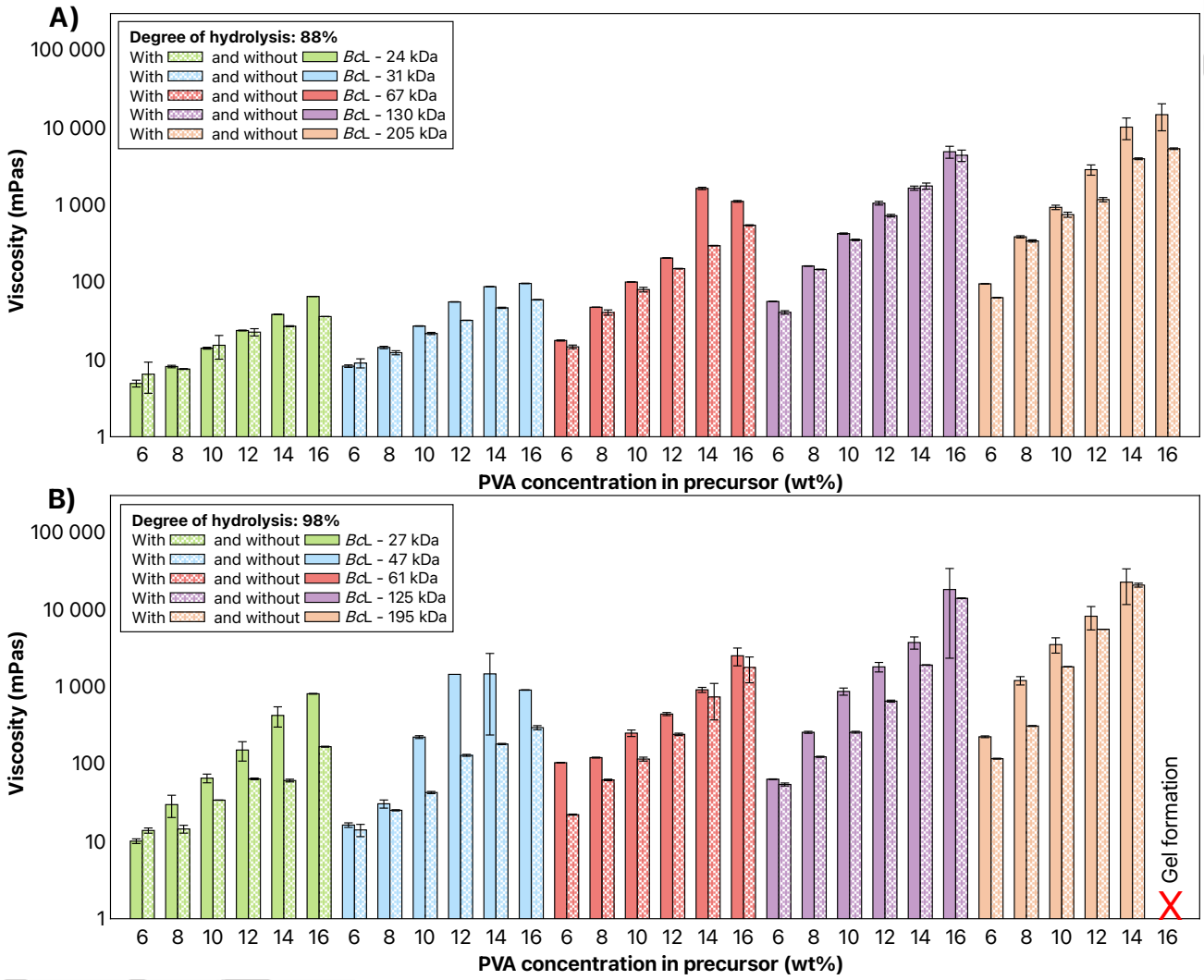

Figure 5. Viscosity values (mPas) and their standard deviation as a function of the degree of hydrolysis (DoH): A) DoH 88 % and B) DoH 98 %. Average molecular weight and PVA concentration of the PVA used in the precursor solutions, determined from rheological studies of enzyme-free and enzyme-containing PVA-based precursor solutions. The samples were analyzed at 25.0 °C. Dynamic viscosity values were calculated at 10 s^{-1} shear rate (γ).

3.2. Entrapment of *Bc*L in PVA nanofibers

A nanofibrous matrix of optimal quality, i.e., a uniform, intact fibrous morphology and a narrow fiber diameter distribution, is essential to develop a robust carrier for biocatalysts. The precursor made from the mixture of polymer and enzyme molecules is formed to a solid, nanofibrous mat, which means a polymer/enzyme two-phase system. Therefore, we first examined the optimal voltage (*U*) and dosing rate values (*V*) required for this, as well as the collector-emitter distance (*l*). The optimum voltage was determined by continuously increasing the supply-generated voltage and searching for the lowest *U* value at which the first fiber exited the polymer droplet on the emitter tip, after which the fiber formation became continuous. It was important to utilize the lowest possible voltage for electrospinning because the lipase to be immobilized is sensitive to extreme environmental conditions,

so an excessively high voltage electric field could induce unwanted structural changes in the enzyme, reducing its catalytic efficiency.[157] The applied voltage typically ranged from 12 to 14 kV. When choosing the collector-emitter distance, the following aspects were considered: If the distance is too large, the polymer particles can only reach the collector under high voltage, and this should be avoided for the reasons described above. If the distance from the emitter is too short, the polymer does not spend enough time in the air to elongate (its specific surface area does not increase) enough to dry out before it reaches the collector so that a droplet is formed on the collector instead of fibers. Typically, *l* between 12 and 16 cm was used. The optimal dosing rate was achieved when the volume of the droplet at the emitter's tip stabilized during continuous dosing and withdrawal via fiber formation, at around 20 µL min^{-1}.

All PVA precursor solutions (see Figure 3) were submitted to electrospinning experiments with a setup for proper fiber formation parameters (*U*, *I*, *V*). The formed structures were examined by scanning electron microscopy. Based on their morphology, the samples were divided into three distinct groups, as shown in Figure 6. In the case of unsuccessful fiber formations, only spray-dried PVA particles could be observed (Figure 6, ○), heterogeneous matrices with a mixture of fiber-like structures and beads could mean a transition stage between the bad and optimal cases (Figure 6, ○), and uniform nanofibers without heterogeneities could be labeled as optimal fibrous products (Figure 6, ○).

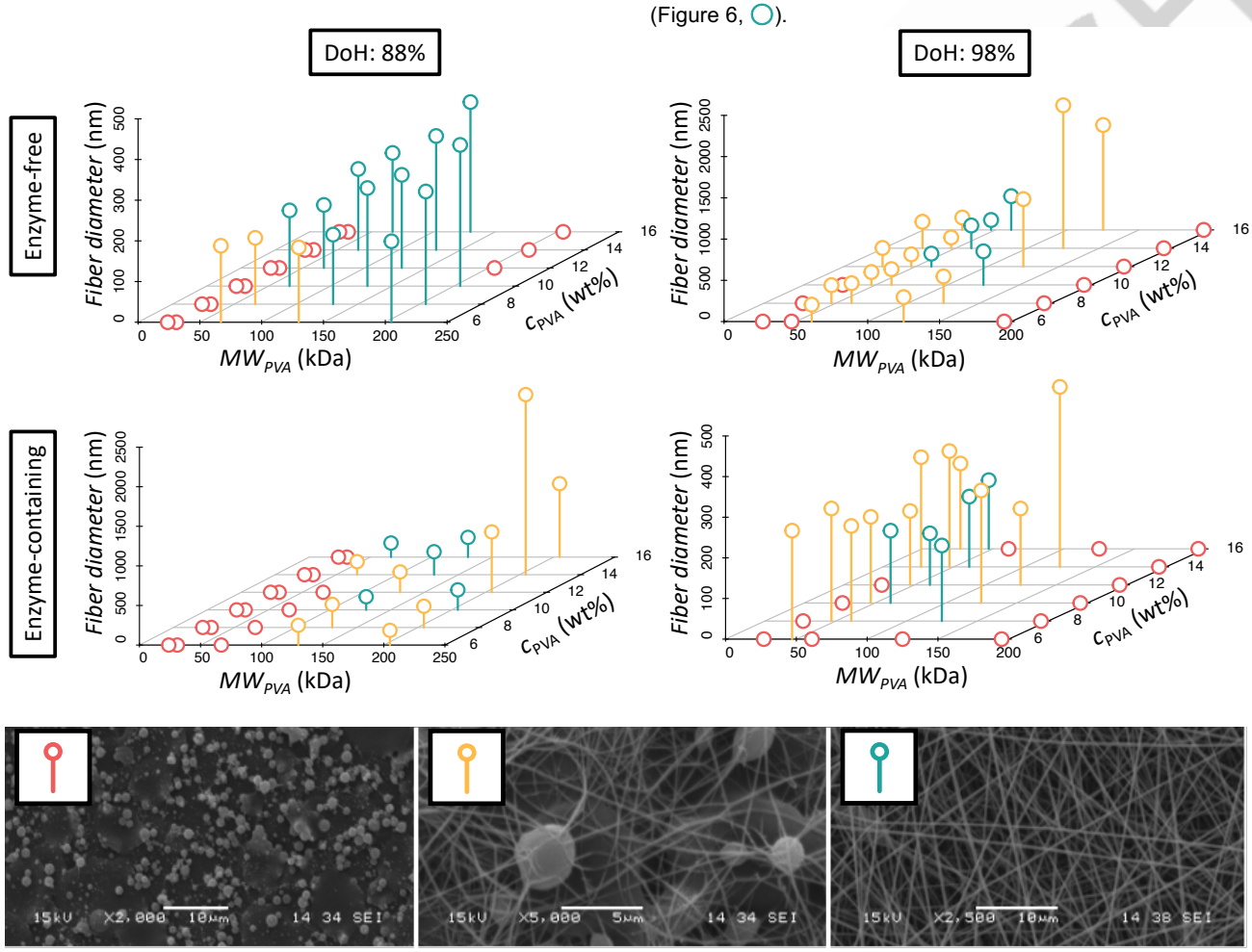

Figure 6. The mean fiber diameters determined during the optimization of the precursor solution of enzyme-free and enzyme-containing PVA nanofibers as a function of the degree of hydrolysis (DoH) and the average molecular weight (MW_{PVA}) of the applied PVA, as well as the concentration of the precursor solution (c_{PVA}). After the electrospinning process, samples were examined by scanning electron microscopy (SEM) at the magnification of 5,000× by evaluating 100-100 point pairs recorded on SEM images. The diameters in this figure were determined only based on the fibrous parts of the samples, and the parts with beads or other deformations were excluded from the evaluation. The colors of the markers in the figure refer to the typical morphologies of the nanofibers that were encountered during the electrospinning experiments, which are also visualized at the bottom of the figure. ○: No fibers were formed from the tested solution due to the properties of the solution fiber formation was not technically feasible. ○: Fiber formation was technically feasible, but the morphology of the fibers was not ideal, the standard deviation of the fiber diameter was too large. ○: Fiber formation was feasible, the morphology of the fibers formed was optimal, and the standard deviation of the fiber diameter was sufficiently small.

The evaluation of electrospun products extended beyond visual morphological categorization, encompassing a qualitative comparison of their average fiber diameters, helped by software analysis of SEM images of the various samples. Based on the results summarized in Figure 6, as the molecular weight of the polymer and the concentration of the polymer solution increase, the diameter of the formed fibers increases monotonically to a limit, after which fiber formation is no longer feasible. The

explanation of this phenomenon is that as the chain length and concentration of the polymer molecules dissolved in the precursor mixture increase, the number of physical ("entanglement") and intermolecular chemical interactions (dipole-dipole and hydrogen bonds) among the polymer chains increases greatly. Consequently, the viscosity of precursor solutions also increases significantly, as seen above (Figure 5), which has been reported to contribute to increased fiber diameters.[150, 151] High viscosity exceeding a critical threshold can make it challenging to produce precursor solutions (achieving adequate homogeneity during the dissolution process), also the excessive interaction of polymer molecules may make it challenging to produce a steady-state material flow from the precursor droplet sitting on the tip of the emitter during electrospinning, even with the application of high voltages (25-30 kV). Furthermore, extremely viscous polymer solutions may not even reach the emitter through the feed tube during pumping, creating a technical barrier to fiber formation.[151] It is also important to note, that fibrous products with uniform structure could be formed from the fully hydrolyzed forms of low molecular weight PVAs, while at larger molecular weights the partially hydrolyzed PVAs performed substantially better. The most likely explanation for this, as mentioned before is that the polymer-polymer interaction between fully hydrolyzed chains is stronger, which in terms of electrospinning is advantageous at low molecular weights but disadvantageous at the higher *MW* region. Results showed that the addition of the enzyme made the formation of a regular fibrous structure and the practical implementation of fiber formation much more difficult. The conditions for optimal fiber formation are stricter compared to enzyme-free nanofibers. The most likely explanation for this observation is related to the previous discussion, in which the effect of enzyme-polymer interactions on the precursor solution viscosity was outlined. The enzyme-polymer interactions are likely to influence key solution properties (such as viscosity), which are essential for a stable electrospinning process. Variations in these properties may cause problems during fiber formation. By comparing the corresponding green regions in Figure 6, it can be seen that, in many cases, the average diameter of the enzyme-filled fibers was smaller than that of the enzyme-free fibers. The reduction in precursor viscosity following enzyme addition (shown in Figure 5) is most likely the main effect leading to thinner fibers during the electrospinning process. Another possible factor contributing to the decreased fiber diameter could be the interactions of the enzyme and poly(vinyl alcohol), where enzyme-PVA complexes formed in the precursor solution are encapsulated within the fibers during electrospinning, stabilized by strong intermolecular polar interactions[158], leading to a tighter structure. Regarding Figures 5 and 6, we can conclude that the fiber-forming apparatus for the experiments is not suitable for satisfactory fiber-forming of solutions with viscosities smaller than 0.1 Pas or larger than 5 Pas (of course, this threshold may vary with different technological parameters). Our experiments have also shown that in addition to the specific viscosity value, the homogeneity of the precursor solutions (the standard deviation of viscosity values) plays a decisive role in the formation of fiber structures.

Determining the enzyme distribution in the electrospun nanofibers is an important issue, thus, Raman spectroscopy was applied. A sample holder glass slide was coated with a slice of aluminum foil containing electrospun nanofibers and put under the Raman microscope to ensure a smooth and even surface to prevent focusing mistakes during analysis. The low spectral background and lack of spectral characteristics, which may interfere with the measurement, were further benefits of using the aluminum foil. A high intensity peak can be seen in the vibrational bands of carbonyl stretching in the amide I region (1600–1700 cm^{-1}), which is characteristic for the secondary structure of proteins. The distinctive amide I band in the Raman spectra is mostly caused by the peptide group of enzyme' C-O stretching vibration. The α-helix (1663 cm^{-1}) and β-strands (1702 cm^{-1}) related signals can be easily distinguished. Sharp peaks between 1420 and 1508 cm^{-1} in Raman spectra are related C-H bending in the protein structure. The amide III region of enzymes is also visible at 1100-1147 cm^{-1}, which corresponds to peptide bond N-H bending and C-N stretching. After the first structural analysis of the lipase, Raman mapping was used to examine how the enzymes were distributed in the various nanofibers. For the identification of enzymes in the PVA nanofibers, the Raman spectrum of the non-entrapped *Bc*L enzyme was used as a reference. The occurance of enzyme-related frequencies is shown in the chemical maps, which represents statistical distribution of the specific chemical entities. The different colors in the chemical maps (Figure 7) show changes in relative intensity of the lipase-specific spectrum components. The blue areas on the map represent the sections of the map where the spectral resolution contains spectra that are distinctive for non-lipase components, while the red areas indicate significant presence of the enzyme, and the green areas reveal a mixed composition. The lipase is indeed embedded inside the nanofibers during the fiber formation process. Furthermore, it can be concluded that the distribution of proteins in the fibers is random and does not correlate with the type of the PVA used or the concentration of the precursor solution.

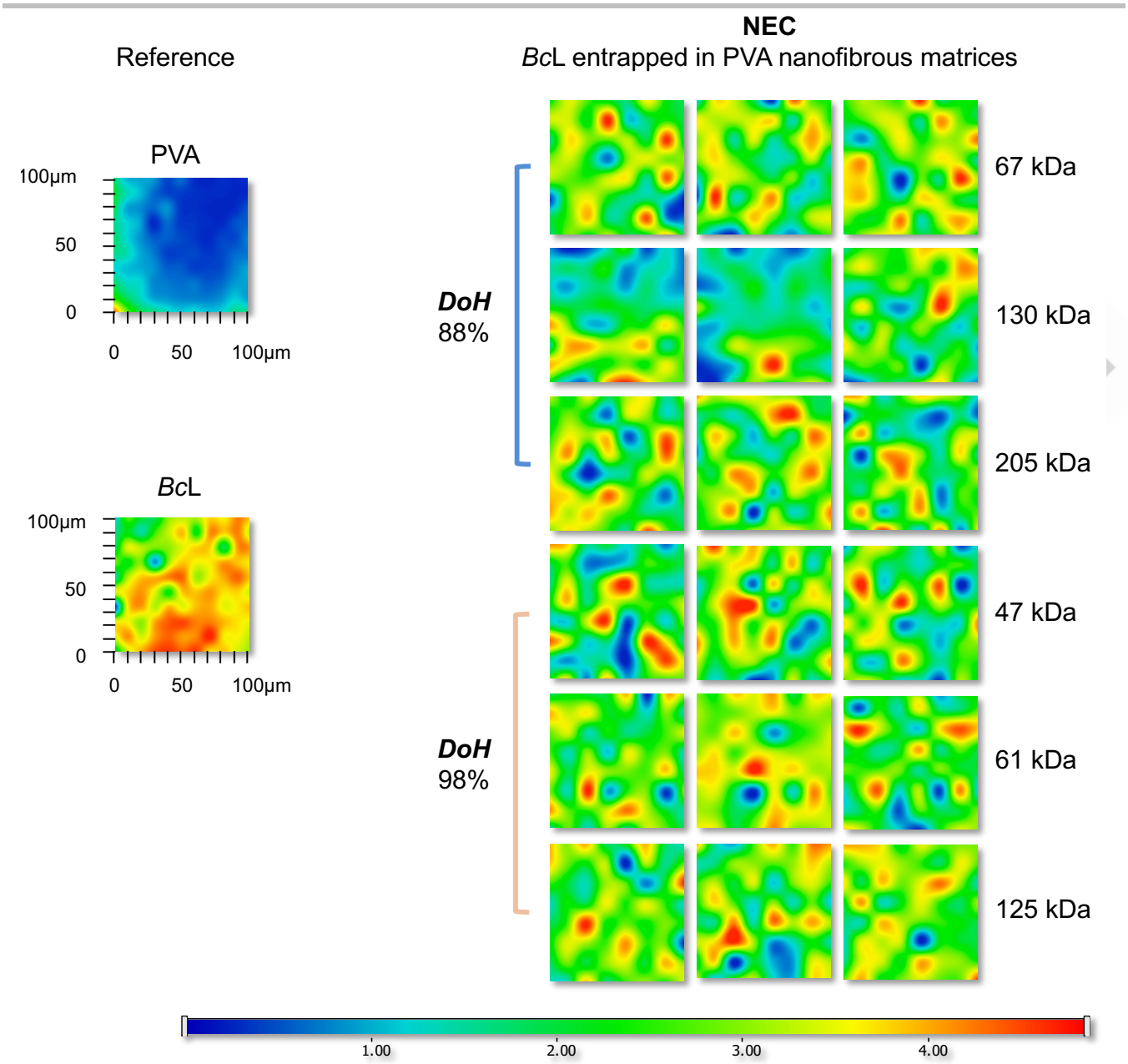

Figure 7. Raman maps of NEC (Nanofibrous Enzyme Catalysts): *Bc*L enzyme-containing PVA nanofibrous matrices, electrospun from PVA polymers with various molecular weights and degrees of hydrolysis (DoH). The location of *Bc*L enzyme is indicated with red, their absence with blue. The green regions indicate mixed compositions.

3.3. Effect of PVA on biocatalytic properties of *Bc*L enzyme entrapped in PVA nanofibers

To compare the effect of PVA polymers with different degrees of hydrolysis and molecular weights on the activity of an immobilized enzyme, *Bc*L lipase entrapped in electrospun PVA nanofibers AS NEC was studied as biocatalyst in the transesterification of *rac*-**2** (see in Section 2.8) in organic solvents (*n*-hexane:MTBE, 2:1, V:V). By the analysis of reaction compounds, two basic biocatalytic parameters were determined, the enantiomeric excess calculated for the main product ($ee_{(R)\text{-}1}$, %) related to the enzyme selectivity, while the apparent activity was characterized by the (Y_A, %, which shows the yield of specific enzyme activities compared to the native enzyme.

Table 1. Investigation of *Bc*L entrapped in PVA nanofibers in the lipase catalyzed transesterification of *rac*-**2**. Test reactions were carried out at 30 °C under constant shaking. The table summarizes the results obtained by gas chromatography of samples taken after reaction time of 24 h. For each sample, the enantiomeric excess of (*R*)-2-octyl acetate ($ee_{(R)\text{-}1}$, %), and the activity yield (Y_A, %, $U_{E,\text{immobilized enzyme}} \times U_{E}^{-1},_{\text{native enzyme}}$, where $U_E = n_s \times c \times (t \times m_E)^{-1}$ in $U \times g^{-1}$ is the specific enzyme activity, described in Section 2.9) were determined as functions of the degree of hydrolysis (DoH) and molecular weight of PVA (MW_{PVA}), as well as the concentration of PVA in the precursor solution (c_{PVA}, %)..

DoH (%)	MW_{PVA} (kDa)	c_{PVA} (wt%)	$ee_{(R)\text{-}1}$ (%)	Y_A (%)
88	67	16	77.4 ± 0.1	97 ± 11
	130	10	77.3 ± 0.5	161 ± 5
	130	14	79.2 ± 0.1	168 ± 11
	130	16	85.0 ± 0.1	47 ± 2
	205	10	79.9 ± 0.7	125 ± 1
98	47	16	77.7 ± 0.1	433 ± 22
	61	10	73.1 ± 0.1	614 ± 37
	61	12	71.4 ± 0.1	1000 ± 67
	61	14	73.2 ± 0.1	907 ± 98
	125	8	74.2 ± 0.1	760 ± 24

Table 1 showes that *Bc*L embedded in the fibrous formulation exhibit higher specific activity than its native form, as Y_A values are larger than 100% in most cases. Furthermore, the Y_A values of *Bc*L encapsulated in nanofibers using fully hydrolyzed PVA exceeded that of found for *Bc*L embedded in matrices made of partially hydrolyzed PVA. The apparent activity of the *Bc*L entrapped in the electrospun PVA nanofibers has maxima either on the molecular weight (MW_{PVA}) or on the concentration (c_{PVA}) of the precursor PVA. This behavior is most likely due to variations in the free volume of nanofibrous matrices, since when submerged in the reaction media, the nanofibrous PVA matrix does not dissolve but remains around the *Bc*L. The influence of molecular weight of the precursor polymer on the structure of highly porous materials has been demonstrated for both electrospun nanofibers[159] and extrusion drew membranes.[160] In both cases, larger molecular weights were shown to contribute to increased porosity. The catalytic activity of entrapped enzymes is heavily dependent upon the free volume and architecture of the supporting matrix. Enclosure within the polymer matrix has been reported to offer structural stability to the enzymes. Proteins larger than the free volume of the support matrix become confined within, creating a protective microenvironment, improving catalytic activity. In case of too small free volume enzyme activity may be constrained by substrate diffusion and access to the active site. The diverse range of free volumes and interconnectivity within the matrix may render some entrapped enzymes inaccessible to substrate diffusion, thus diminishing catalytic activity.[161] Furthermore, our work has demonstrated that increasing the MW_{PVA} and c_{PVA} leads to a growth in fiber diameter. As the nanofibrous matrix limits the substrate diffusion, the increase in the size of the fiber presumably contributes to the apparent lower catalytic activity at higher molecular weights and precursor concentrations.

Immobilization of *Bc*L notably enhanced its apparnet activity, likely attributed to favorable interactions between the matrix polymer and the embedded protein. PVA chains may favorably stabilize or lock the active conformation of the enzyme, facilitating substrate binding. The formation of such interactions is expected to cause changes in the thermal properties of the system, which can be examined by differential scanning calorimetry (DSC).[162] Consequently, we conducted calorimetric investigation was performed on the most active NEC biocatalysts listed in Table 1. Data in Figure 8 revealed that the immobilization of *Bc*L within PVA nanofibers has led to a consistent decrease in the measured glass transition temperatures. Specifically, for partially hydrolyzed PVA, the transition temperatures (T_g) have shifted from the 30-40°C range observed in enzyme-free nanofibers to a range of 25-35°C following enzyme immobilization. Similarly, for fully hydrolyzed PVA, the transition temperatures have changed from the 30-40°C range to a range of 25-40°C upon enzyme immobilization. A notable correlation between the glass transition temperature (T_g) and the specific enzyme activity (U_E) of the nanofibrous lipases is visible in Figure 8. Specifically, an increase in T_g corresponds to a concomitant enhancement in specific enzyme activity. An interesting observation is noted around the temperature of the conducted test reaction (30°C), where a remarkable increase is observed in the measured specific enzyme activities. This suggests that samples in the glassy state, characterized by T_g values exceeding 30°C, contribute to higher activities compared to samples in the rubber elastic state with T_g values below 30°C. This finding may indicate the beneficial effect of the more rigid matrix structure on the enzyme conformation, since more rigid matrices could conserve the proper structural l state of enzymatic activity.

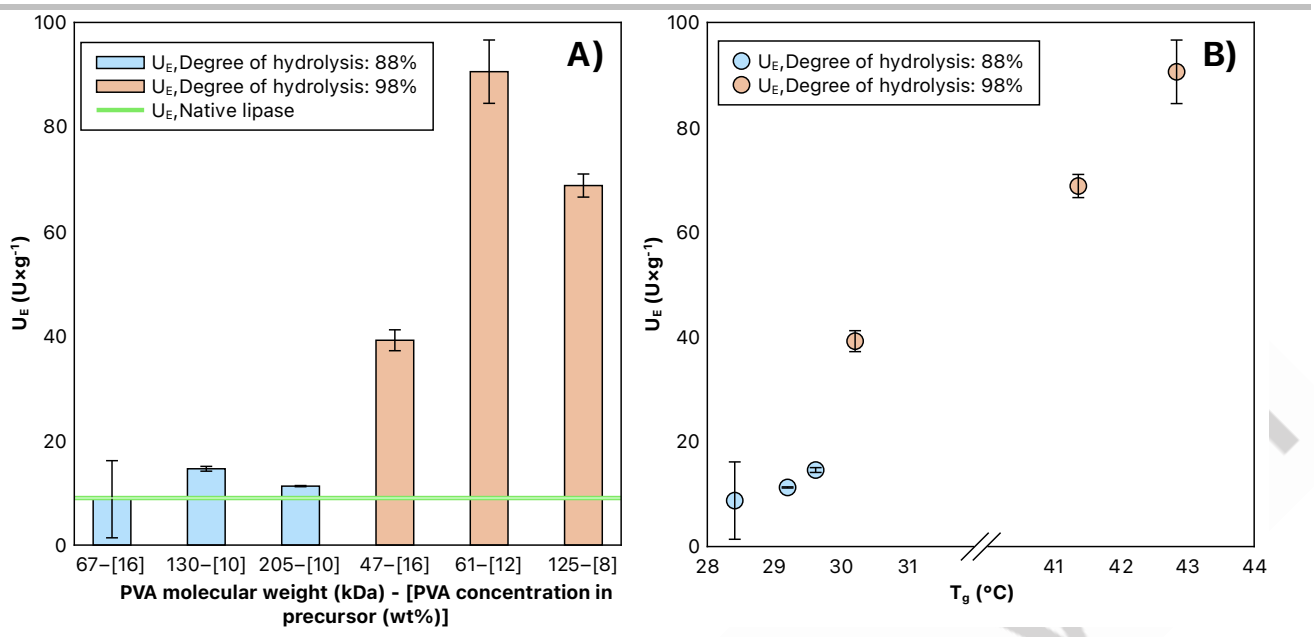

Figure 8. A) Specific enzyme activities (U_E, U×g^{-1}) of *Bc*L entrapped in PVA nanofibers compared to the activity of native *Bc*L. **B)** Correlation between glass transition temperatures (T_g, °C) and U_E values. To determine T_g values, samples were heated from −20 oC to 150 °C in 2 cycles at 10 °C min^{-1}. T_g values were read during the first heating. U_E values were determined from the transesterification between *rac*-**2** and VA. Test reactions were carried out at 30 °C under constant shaking. The results were obtained by gas chromatography of samples taken 24 h after the start of the reactions.

3.4. Results of molecular docking simulations

Nanobiocatalysts immobilized at optimal conditions showed significantly higher activity than the native enzyme, suggesting that the immobilization process may provide an additional stabilizing or bioimprinting effect. We aimed to explore the molecular background of this phenomenon with computational methods. The computational investigation of interactions between polymer and protein chains is a difficult task, however the development of a simplified methodology could enable to test the hypothesis. Molecular docking simulations with constraints that allowed us to interpret the results as an estimation on how PVA polymer chains may interact with *Bc*L. As for the receptors, an *apo* and an inhibitor complexed structure of *Bc*L were used (PDB IDs 2LIP and 1YS1). During the docking process, a relatively large grid box was applied to allow interactions of PVA-mimicking oligomers not only with the active site pocket but the surface of the enzyme as well. The docked ligands were PVA-mimicking oligomers consisting of 12, 15 and 19 monomer units as ligands. To mimic the different DoHs (88% and 98%) were investigated, acetyl groups were added to the ligands accordingly. In all the conducted simulations, the docked poses of PVA ligands accumulated in the active center, indicating that PVA was able to interact with the active center forming residues and behaved as a bioimprinting agent. Docking results were analyzed and visually evaluated as specified in Section 2.11. The developed simplified PVA-mimicking oligomer methodology (illustrated by examples depicted in Figure 9) allowed us to filter and keep only polymer chain mimicking positions for further investigation. Panel 9A shows an example for a position that was considered as polymer mimicking ligand (both ends of the ligand chain are out of AS). Several docking poses (when both ends of the ligand chain were in the AS, as shown in Panel 9B; or even if only one end was in the AS) were discarded as inadequate to mimic polymer binding. Panel 9C demonstrates how the active center forming residues of BcL can interact with a part of a PVA polymer through hydrogen bonds. In the case of shorter ligands (12 and 15 monomers), only a few docked positions could be interpreted as polymer mimicking results due to the shortness. Thus, the longest investigated PVA-mimicking oligomers (consisting of 19 monomers with length limited by the selected computational setup) were the most suitable for further evaluation. The affinity results of the 19 monomer-long PVA ligands in the docking runs with two different structural states of *Bc*L (apo- and ligand-containing) are visualized on Figure 10. Docking results showed that PVA with DoH either of 88% or of 98% could interact with the active side residues of BcL. Although PVA with 88% DoH appeared to have higher affinity to the fully open but apo *Bc*L structure, but the affinity results with the two types of ligands (mimicking DoH 88% or 98%) were alike in docking into the ligand-complexed structure of *Bc*L (corresponding better to the ligand binding active state of the enzyme).

These results and the visual inspection of the docked positions revealed several secondary interactions between the polymer matrix and the enzyme, further strengthening our assumption considering PVA chains as bioimprinting agents for *Bc*L. Bioimprinting is a useful approach to preserve or even enhance the catalytic performance of enzymes during drying or immobilization processes by stabilizing the active conformation of the active center with an appropriate bioimprinting molecule.[163] This beneficial effect has been demonstrated for various lipases in the past with a wide plethora of compounds such as substrates, products[164, 165], ionic and non-ionic detergents[163, 166, 167], or silica sol-gel precursors.[168] Our study shows that parts of larger

polymers can exhibit bioimprinting effects as well, and that careful selection and optimization of immobilization parameters can result in highly capable biocatalysts.

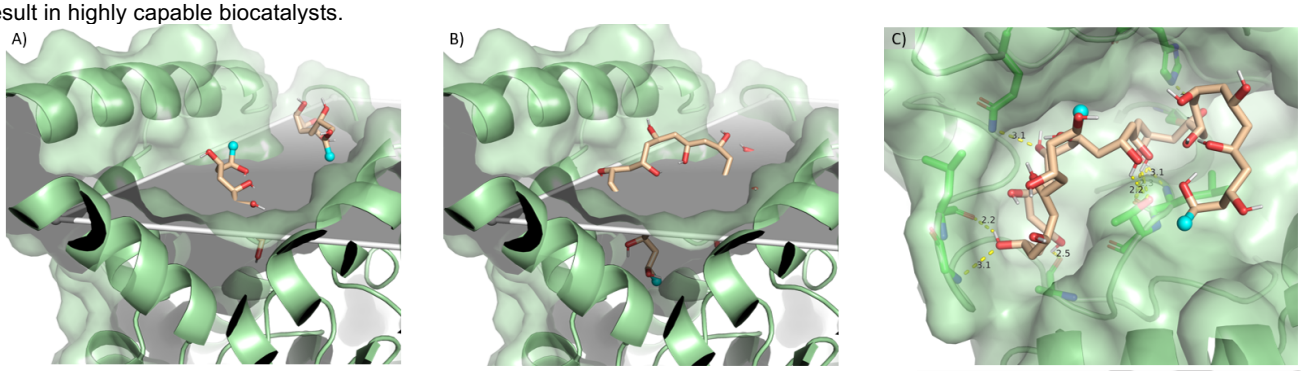

Figure 9. Representative docking results of a 19 monomer-long PVA chain-mimicking ligand (pale pink, ending C atoms are marked with cyan spheres) with experimental structure of *Bc*L (PDB ID: 2LIP) as receptor (green). Docking simulation and visualization were carried out with AutoDock Vina program via DockingPie plugin in PyMol. A) A ligand pose that can be considered as mimic of a possible interaction of a longer PVA polymer chain (the ends of the ligand—marked with cyan spheres—are out of the plane that covers the active center). B) A ligand pose that was considered as not representing a part of a longer polymer chain (ending atoms of the docked ligand were positioned deeply inside the active site pocket). C) Polar interactions between a docked PVA chain-mimicking ligand and the active site residues of *Bc*L.

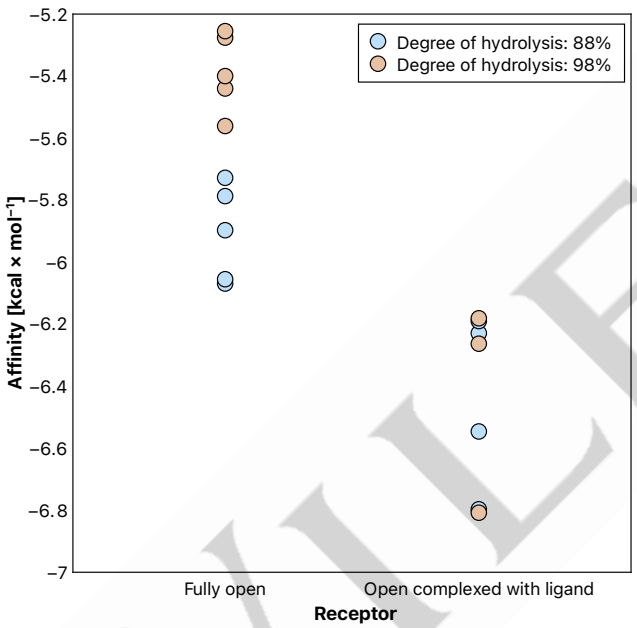

Figure 10. Affinity results of poses of PVA ligand with different degrees of hydrolysis (DoH) in molecular docking towards the different structures of BcL. Docking was carried out with AutoDock Vina program via DockingPie Plugin in PyMol, results were plotted in R.

4. Summary and Outlook

This comprehensive study details the limitations of electrospinning from aqueous precursor solutions of commercially available poly(vinyl alcohol) (PVA) of different molecular weights and degrees of hydrolysis of as well as the enzyme entrapping ability of the obtained fibrous nanostructures. Furthermore, it reveals relationships between the catalytic activity of the immobilized model enzyme (*Burkholderia cepacia* lipase, *Bc*L) and the conditions of fiber formation. The effects of the molecular weight, degree of hydrolysis, and concentration of PVA precursor solution for the fiber morphology and the rheological properties of the solutions were investigated in detail. The fiber-forming ability of PVA has been mapped over a wide range, and its technological limitations have been identified. In the electrospinning process applicable for *Bc*L entrapment resulting in immobilized nanofibrous biocatalyst, the effect of the presence of the enzyme on the fiber structure and solution viscosity was investigated. The kinetic resolution processes selected as test reactions revealed that the degree of hydrolysis, molecular weight, and precursor concentration of PVA significantly affected the biocatalytic activity of the nanofiber-embedded lipase. The differential scanning calorimetry (DSC) analysis revealed a correlation between the glass transition temperature (T_g) of the nanofibers and the specific enzyme activity (U_E), indicating that samples with higher T_g values exhibit increased enzyme activity. This suggests that PVA chains effectively stabilize the enzyme within the nanofibrous matrix, facilitating optimal conditions for catalytic performance. By careful selection of the proper conditions for fiber formation and entrapment, a nanofibrous immobilized *Bc*L biocatalyst formulation could be produced with a specific activity being more than ten times higher than that of the native model lipase, *Bc*L. Furthermore, properly simplified computational docking simulations aiming to model the interaction between PVA and *Bc*L revealed that PVA chains may act as bioimprinting agents, enhancing the enzyme's stability and catalytic performance, offering insights into the optimization of nanobiocatalyst immobilization for various applications.

Acknowledgements

This research has been supported by the National Research Development and Innovation (NRDI) Fund via grant FK-137582 (D.B.W.) and 2021-1.1.4-GYORSÍTÓSÁV-2022-00059. D.B.W. also acknowledges the János Bolyai Research Scholarship of the Hungarian Academy of Sciences (BO/00175/21). The research

reported in this paper is part project no. TKP-9-8/PALY-2021 has been implemented with the support provided by the Ministry of Culture and Innovation of Hungary from the National Research, Development and Innovation Fund, financed under the TKP2021-EGA funding scheme. The support of the Servier-Beregi Fellowship (G.T.).

Keywords: Nanofiber • Polyvinyl Alcohol (PVA) • Biocatalysis • Enzyme Immobilization • Electrospinning

References

[1] N. S. Punekar, *ENZYMES: Catalysis, Kinetics and Mechanisms*; Springer Singapore: Singapore, **2018**.

[2] G. Banerjee, J. S. Scott-Craig, J. D. Walton, *Bioenergy Res.* **2010**, 3, 82–92.

[3] S. Kara, J. H. Schrittwieser, F. Hollmann, M. B. Ansorge-Schumacher, *Appl. Microbiol. Biotechnol.***2014**, 98, 1517–1529.

[4] H. Vaghari, H. Jafarizadeh-Malmiri, M. Mohammadlou, A. Berenjian, N. Anarjan, N. Jafari, S. Nasiri, *Biotechnol. Lett.* **2016**, 38, 223–233.

[5] T. Palmer, P. L. Bonner, *Enzymes: Biochemistry, Biotechnology, Clinical Chemistry*; Elsevier, **2007**.

[6] H. Bisswanger, *Perspect. Sci.* **2014**, 1, 41–55.

[7] K. T. Sriwong, T. Matsuda, *Org. Process Res. Dev.* **2022**.

[8] H. H. Nguyen, M. Kim, *Appl. Sci. Converg. Technol.* **2017**, 26, 157–163.

[9] R. Das, M. Talat, O. N. Srivastava, A. M. Kayastha, *Food Chem.* **2018**, 245, 488–499.

[10] M. Bilal, H. M. Iqbal, *Int. J. Biol. Macromol.* **2019**, 130, 462–482.

[11] J. G. S. Mala, S. Takeuchi, *Anal. Chem. Insights.* **2008**, 3, 551.

[12] H. Jooyandeh, K. Amarjeet, K. S. Minhas, *J. Food Sci. Technol.* **2009**, 46, 181–189.

[13] F. L. Oliveira, S. C. Rumsey, E. Schlotzer, I. Hansen, Y. A. Carpentier, R. J. Deckelbaum, *J. Parenter. Enter. Nutr.* **1997**, 21, 224–229.

[14] A. Houde, A. Kademi, D. Leblanc, *Appl. Biochem. Biotechnol.* **2004**, 118, 155–170.

[15] M. S. H. Akash, K. Rehman, S. Chen, *Polym. Rev.* **2015**, 55, 371–406.

[16] L.-L. Zhu, C.-T. Zhu, M. Xiong, C.-Q. Jin, S. Sheng, F.-A. Wu, J. Wang, *J. Chem. Technol. Biotechnol.***2019**, 94, 1670–1678.

[17] T. Volova, E. Kiselev, I. Nemtsev, A. Lukyanenko, A. Sukovatyi, A. Kuzmin, G. Ryltseva, E. Shishatskaya, *Int. J. Biol. Macromol.* **2021**, 182, 98–114.

[18] A. N. Storey, W. Zhang, J. F. Douglas, F. W. Starr, *Macromolecules* **2020**, 53, 9654–9664.

[19] A. Dwevedi, *Basics of Enzyme Immobilization*; **2016**.

[20] Y. Liu, J. Y. Chen, *J. Bioact. Compat. Pol.* **2016**, 31, 553–567.

[21] M. L. Verma, S. Kumar, A. Das, J. S. Randhawa, M. Chamundeeswari, *Environ. Chem. Lett.* **2020**, 18, 315–323.

[22] P. Zucca, R. Fernandez-Lafuente, E. Sanjust, *Molecules* **2016**, 21, 1577.

[23] S. J. Chakraborty, *J. Carbohydr. Chem.* **2017**, 36, 1–19.

[24] D. Wang, W. Jiang, *Int. J. Biol. Macromol.* **2019**, 126, 1125–1132.

[25] L. E. Nielsen, *J. Macromol. Sci., Part C* **1969**, 3, 69–103.

[26] N. Bhardwaj, S. C. Kundu, *Biotechnol. Adv.* **2010**, 28, 325–347.

[27] A. Jaworek, A. T. Sobczyk, *J. Electrostat.* **2008**, 66, 197–219.

[28] N. Rajput, *Int. J. Adv. Eng. Technol.* **2015**, 7, 1806.

[29] H. Yabu, T. Higuchi, K. Ijiro, M. Shimomura, *Chaos* **2005**, 15, 047505.

[30] C. J. M. Rivas, M. Tarhini, W. Badri, K. Miladi, H. Greige-Gerges, Q. A. Nazari, S. A. G. Rodríguez, R. Á. Román, H. Fessi, A. Elaissari, *Int. J. Pharm.* **2017**, 532, 66–81.

[31] S. Haque, B. J. Boyd, M. P. McIntosh, C. W. Pouton, L. M. Kaminskas, M. Whittaker, *Curr. Nanosci.***2018**, 14, 448–453.

[32] U. Jana, S. Pal, G. P. Mohanta, P. K. Manna, R. Manavalan, *Res. J. Pharm. Technol.* **2011**, 4, 1016–1019.

[33] X. L. Liu, E. S. G. Choo, A. S. Ahmed, L. Y. Zhao, Y. Yang, R. V. Ramanujan, J. M. Xue, H. M. Fan, J. J. Ding, *J. Mater. Chem. B* **2014**, 2, 120–128.

[34] J. Martín, J. Maiz, J. Sacristan, C. Mijangos, *Polymer* **2012**, 53, 1149–1166.

[35] T. Ravula, N. Z. Hardin, A. Ramamoorthy, *Chem. Phys. Lipids* **2019**, 219, 45–49.

[36] X. Ji, P. Wang, Z. Su, G. Ma, S. Zhang, *J. Mater. Chem. B* **2014**, 2, 181–190.

[37] S. Nangare, N. Jadhav, P. Ghagare, T. Muthane, *Ann. Pharm. Fr.* **2020**, 78, 1–11.

[38] S. S. Shahriar, J. Mondal, M. N. Hasan, V. Revuri, D. Y. Lee, Y.-K. Lee, *Nanomaterials* **2019**, 9, 532.

[39] X. Wang, B. S. Hsiao, *Curr. Opin. Chem. Eng.* **2016**, 12, 62–81.

[40] M. Gorji, R. Bagherzadeh, H. Fashandi, *Electrospun Nanofibers in Protective Clothing* **2017**.

[41] S. Ramakrishna, *An Introduction to Electrospinning and Nanofibers*; World Scientific: **2005**.

[42] Y. Fan, X. Tian, L. Zheng, X. Jin, Q. Zhang, S. Xu, P. Liu, N. Yang, H. Bai, H. Wang, *Mater. Sci. Eng. C***2021**, 120, 111747.

[43] T. G. Kim, T. G. Park, *Biotechnol. Prog.* **2006**, 22, 1108–1113.

[44] M. K. Ramasubramanian, D. L. Shmagin, *J. Manuf. Sci. Eng.* **2000**, 122, 576–581.

[45] R. V. Gadhave, P. V. Dhawale, *Open J. Polym. Chem.* **2022**, 12, 13–42.

[46] S.-F. Chong, A. A. Smith, A. N. Zelikin, *Small* **2013**, 9, 942–950.

[47] L. S. Peixoto, F. M. Silva, M. A. L. Niemeyer, G. Espinosa, P. A. Melo, M. Nele, J. C. Pinto, *Macromol. Symp.* **2006**, 243, 190–199.

[48] L. Wu, X. Yuan, J. Sheng, *J. Membr. Sci.* **2005**, 250, 167–173.

[49] D. Weiser, P. L. Sóti, G. Bánóczi, V. Bódai, B. Kiss, Á. Gellért, Z. K. Nagy, B. Koczka, A. Szilágyi, G. Marosi, *Tetrahedron* **2016**, 72, 7335–7342.

[50] S. Saallah, M. N. Naim, I. W. Lenggoro, M. N. Mokhtar, N. F. A. Bakar, M. Gen, *Biotechnol. Rep.* **2016**, 10, 44–48.

[51] M. D. A. Porto, J. P. D. Santos, H. Hackbart, G. P. Bruni, L. M. Fonseca, E. da Rosa Zavareze, A. R. G. Dias, *Int. J. Biol. Macromol.* **2019**, 126, 834–841.

[52] E. Shoba, R. Lakra, M. S. Kiran, P. S. Korrapati, *RSC Adv.* **2014**, 4, 60209–60215.

[53] U. D. Kamaci, A. Peksel, *Int. J. Biol. Macromol.* **2020**, 164, 3315–3322.

[54] C. Tang, C. D. Saquing, S. W. Morton, B. N. Glatz, R. Kelly, S. A. Khan, *ACS Appl. Mater. Interfaces***2014**, 6, 11899–11906.

[55] Q. Feng, B. Tang, Q. Wei, D. Hou, S. Bi, A. Wei, *Int. J. Mol. Sci.* **2012**, 13, 12734–12746.

[56] U. D. Kamaci, A. Peksel, *Catal. Lett.* **2021**, 151, 821–831.

[57] E. Baştürk, S. Demir, Ö. Danış, M. V. Kahraman, *J. Appl. Polym. Sci.* **2012**, 127, 349–355.

[58] G. Işık, Y. I. Arabaci Ispirli Doğaç, İ. Deveci, M. Teke, *Mater. Sci. Eng. C* **2019**, 99, 1226–1235.

[59] A. Amani, S. Taghavi, F. Yazdian, S. Mirzababaei, H. Rashedi, M. A. Faramarzi, M. Vahidi, *Biotechnol. Prog.* **2022**, e3282.

[60] I. E. Moreno-Cortez, J. Romero-García, V. González-González, D. I. García-Gutierrez, M. A. Garza-Navarro, R. Cruz-Silva, *Mater. Sci. Eng. C* **2015**, 52, 306–314.

[61] Z. Temoçin, M. İnal, M. Gökgöz, M. Yiğitoğlu, *Polym. Bull.* **2018**, *75*, 1843–1865.

[62] Y. İ. Doğaç, İ. Deveci, B. Mercimek, M. Teke, *Int. J. Biol. Macromol.* **2017**, 96, 302–311.

[63] E. Afshari, S. Mazinani, S.-O. Ranaei-Siadat, H. Ghomi, *Appl. Surf. Sci.* **2016**, 385, 349–355.

[64] B. Unal, E. E. Yalcinkaya, D. O. Demirkol, S. Timur, *Appl. Surf. Sci.* **2018**, 444, 542–551.

[65] K. Nakane, T. Hotta, T. Ogihara, N. Ogata, S. Yamaguchi, *J. Appl. Polym. Sci.* **2007**, 106, 863–867.

[66] P.-Y. Hong, Y.-H. Huang, G. C. W. Lim, Y.-P. Chen, C.-J. Hsiao, L.-H. Chen, J.-Y. Ciou, L.-S. Hsieh, *Int. J. Mol. Sci.* **2021**, 22, 11184.

[67] A. S. Rojas-Mercado, I. E. Moreno-Cortez, R. Lucio-Porto, L. L. Pavón, *Int. J. Biol. Macromol.* **2018**, 118, 2287–2295.

[68] M. Sarathi, N. Doraiswamy, G. Pennathur, *Prep. Biochem. Biotechnol.* **2019**, 49, 695–703.

[69] J.-M. Park, M. Kim, H.-S. Park, A. Jang, J. Min, Y.-H. Kim, *Int. J. Biol. Macromol.* **2013**, 54, 37–43.

[70] S. Haghju, M. R. Bari, M. A. Khaled-Abad, *Carbohydr. Polym.* **2018**, 200, 137–143.

[71] J. Wu, F. Yin, *J. Electroanal. Chem.* **2013**, 694, 1–5.

[72] P. L. Sóti, D. Weiser, T. Vigh, Z. K. Nagy, L. Poppe, G. Marosi, *Bioprocess Biosyst. Eng.* **2016**, 39, 449–459.

[73] L. Ge, Y. sheng Zhao, T. Mo, J. rong Li, P. Li, *Food Control* **2012**, 26, 188–193.

[74] S. E. Rodríguez-deLuna, I. E. Moreno-Cortez, M. A. Garza-Navarro, R. Lucio-Porto, L. L. Pavón, V. A. González-González, *J. Appl. Polym. Sci.* **2017**, 134, 44829.

[75] A. M. Asiri, *J. Electroanal. Chem.* **2017**, 789, 181–187.

[76] J. P. D. Santos, E. da Rosa Zavareze, A. R. G. Dias, N. L. Vanier, *Int. J. Biol. Macromol.* **2018**, 118, 1676–1684.

[77] M. F. Canbolat, N. Gera, C. Tang, B. Monian, B. M. Rao, B. Pourdeyhimi, S. A. Khan, *ACS Appl. Mater. Interfaces* **2013**, 5, 9349–9354.

[78] J. Li, X. Liu, H. Sun, L. Wang, J. Zhang, X. Huang, L. Deng, J. Xi, T. Ma, *IEEE Sensors J.* **2021**, 21, 16078–16085.

[79] R. Xu, R. Tang, Q. Zhou, F. Li, B. Zhang, *Chem. Eng. J.* **2015**, 262, 88–95.

[80] J. Zhu, G. Sun, *React. Funct. Polym.* **2012**, 72, 839–845.

[81] H. Zhu, M. Du, M. Zhang, P. Wang, S. Bao, L. Wang, Y. Fu, J. Yao, *Biosens. Bioelectron.* **2013**, 49, 210–215.

[82] B. Oktay, S. Demir, N. Kayaman-Apohan, *Mater. Sci. Eng. C* **2015**, 50, 386–393.

[83] W. Wang, Q. Zhao, M. Luo, M. Li, D. Wang, Y. Wang, Q. Liu, *ACS Appl. Mater. Interfaces* **2015**, 7, 20046–20052.

[84] K.-O. Kim, B.-S. Kim, *J. Fiber Sci. Technol.* **2017**, 73, 27–33.

[85] C. Tang, C. D. Saquing, P. K. Sarin, R. M. Kelly, S. A. Khan, *J. Membr. Sci.* **2014**, 472, 251–260.

[86] M. Dhawane, A. Deshpande, R. Jain, P. Dandekar, *Sens. Actuators B Chem.* **2019**, 281, 72–79.

[87] C. M. Wu, S. A. Yu, S. L. Lin, *Express Polym. Lett.* **2014**, 8, 8.

[88] J. Liu, J. Niu, L. Yin, F. Jiang, *Analyst* **2011**, 136, 4802–4808.

[89] J. L. García-Zamora, V. Santacruz-Vázquez, M. Á. Valera-Pérez, M. T. Moreira, D. L. Cardenas-Chavez, M. Tapia-Salazar, E. Torres, *Int. J. Environ. Res. Public Health* **2019**, 16, 4917.

[90] S. H. Baek, J. Roh, C. Y. Park, M. W. Kim, R. Shi, S. K. Kailasa, T. J. Park, *Mater. Sci. Eng. C* **2020**, 107, 110273.

[91] B. Coşkuner Filiz, Y. Basaran Elalmis, İ. S. Bektaş, A. Kantürk Figen, *Int. J. Biol. Macromol.* **2021**, 192, 999–1012.

[92] E. Sapountzi, M. Braiek, F. Vocanson, J.-F. Chateaux, N. Jaffrezic-Renault, F. Lagarde, *Sens. Actuators B Chem.* **2017**, 238, 392–401.

[93] Y. Wang, Y. L. Hsieh, *J. Membr. Sci.* **2008**, 309, 73–81.

[94] J. Zeng, A. Aigner, F. Czubayko, T. Kissel, J. H. Wendorff, A. Greiner, *Biomacromolecules* **2005**, 6, 1484–1488.

[95] C. Işik, M. Teke, *J. Polym. Res.* **2022**, 29, 1–17.

[96] P. Tonglairoum, T. Ngawhirunpat, T. Rojanarata, P. Opanasopit, *Pharm. Dev. Technol.* **2015**, 20, 976–983.

[97] J.-A. Park, S.-C. Lee, S.-B. Kim, *J. Mater. Sci.* **2019**, 54, 9969–9982.

[98] Q. Feng, X. Xia, A. Wei, X. Wang, Q. Wei, D. Huo, A. Wei, *J. Appl. Polym. Sci.* **2011**, 120, 3291–3296.

[99] Q. Yang, Y. Yan, X. Yang, G. Liao, D. Wang, H. Xia, *Chem. Eng. J.* **2019**, 372, 946–955.

[100] F. N. Crespilho, R. M. Iost, S. A. Travain, O. N. Jr. Oliveira, V. Zucolotto, *Biosens. Bioelectron.* **2009**, 24, 3073–3077.

[101] J. F. Zhan, S. T. Jiang, L. J. Pan, *Brazilian J. Chem. Eng.* **2013**, 30, 721–728.

[102] E. Piacentini, M. Yan, L. Giorno, *J. Membr. Sci.* **2017**, 524, 79–86.

[103] M. A. Nunes, H. Vila-Real, P. C. Fernandes, M. H. Ribeiro, *Appl. Biochem. Biotechnol.* **2010**, 160, 2129–2147.

[104] A. Dinçer, A. Telefoncu, *J. Mol. Catal. B: Enzym.* **2007**, 45, 10–14.

[105] S. Zuo, Y. Teng, H. Yuan, M. Lan, *Sens. Actuators B: Chem.* **2008**, 133, 555–560.

[106] L. Y. Jun, N. M. Mubarak, L. S. Yon, C. H. Bing, M. Khalid, P. Jagadish, E. C. Abdullah, *Sci. Rep.***2019**, 9, 1–15.

[107] M. D. Stanescu, M. Fogorasi, B. L. Shaskolskiy, S. Gavrilas, V. I. Lozinsky, *Appl. Biochem. Biotechnol.***2010**, 160, 1947–1954.

[108] H. Jia, F. Huang, Z. Gao, C. Zhong, H. Zhou, M. Jiang, P. Wei, *Biotechnol. Rep.* **2016**, 10, 49–55.

[109] A. Idris, N. A. M. Zain, M. S. Suhaimi, *Process Biochem.* **2008**, 43, 331–338.

[110] B. D. S. Silva, C. J. Ulhoa, K. A. Batista, M. C. D. Medeiros, R. R. da Silva Filho, F. Yamashita, K. F. Fernandes, *Carbohydr. Polym.* **2012**, 89, 964–970.

[111] S. Gupta, C. R. Prabha, C. N. Murthy, *J. Environ. Chem. Eng.* **2016**, 4, 3734–3740.

[112] R. Dave, D. Madamwar, *Process Biochem.* **2006**, 41, 951–955.

[113] N. A. M. Zain, S. M. Suardi, A. Idris, *Biochem. Eng. J.* **2010**, 50, 83–89.

[114] L.-S. Zhang, W. zhong Wu, J. long Wang, *J. Environ. Sci.* **2007**, 19, 1293–1297.

[115] R. Jovanovic-Malinovska, P. Fernandes, E. Winkelhausen, L. Fonseca, *Appl. Biochem. Biotechnol.***2012**, 168, 1197–1211.

[116] S. Idris, N. H. Azeman, N. A. N. Azmy, C. T. Ratnam, M. A. Mahdi, A. A. A. Bakar, *Sens. Actuators B: Chem.* **2018**, 273, 1404–1412.

[117] J. Kumar, S. F. D'Souza, *Talanta* **2008**, 75, 183–188.

[118] J. Bergamasco, M. V. de Araujo, A. de Vasconcellos, R. A. L. Filho, R. R. Hatanaka, M. V. Giotto, D. A. Aranda, J. G. Nery, *Biomass Bioenergy* **2013**, 59, 218–233.

[119] Y. Yang, H. A. Chase, *Biotechnol. Appl. Biochem.* **1998**, 28, 145–154.

[120] C. S. Pundir, B. S. Singh, J. Narang, *Clin. Biochem.* **2010**, 43, 467–472.

[121] B. M. Bonine, P. P. Polizelli, G. O. Bonilla-Rodriguez, *Enzyme Res.* **2014**, 2014.

[122] M. Bilal, T. Rasheed, H. M. Iqbal, H. Hu, W. Wang, X. Zhang, *Int. J. Biol. Macromol.* **2017**, 105, 328–335.

[123] M. Sogani, N. Mathur, P. Bhatnagar, P. Sharma, *Int. J. Environ. Sci. Technol.* **2012**, 9, 119–127.

[124] Y.-T. Zhao, K. Zhang, J. Zeng, H. Yin, W. Zheng, R. Li, A. Ding, S. Chen, Y. Liu, W. Wu, *Enzyme Microb. Technol.* **2022**, 157, 110017.

[125] D. F. Neri, V. M. Balcão, R. S. Costa, I. C. Rocha, E. M. Ferreira, D. P. Torres, L. R. Rodrigues, L. B. C. Jr, J. A. Teixeira, *Food Chem.* **2009**, 115, 92–99.

[126] V. Singh, D. Singh, *Process Biochem.* **2013**, 48, 96–102.

[127] C. Chao, H. Guan, J. Zhang, Y. Liu, Y. Zhao, B. Zhang, *Water Sci. Technol.* **2018**, 77, 809–818.

[128] S. K. Jha, A. Topkar, S. F. D'Souza, *J. Biochem. Biophys. Methods* **2008**, 70, 1145–1150.

[129] K. C. Badgujar, B. M. Bhanage, *Process Biochem.* **2015**, 50, 1224–1236.

[130] J. Zang, S. Jia, Y. Liu, S. Wu, Y. Zhang, *Catal. Commun.* **2012**, 27, 73–77.

[131] Y. N. Martínez, I. Cavello, R. Hours, S. Cavalitto, G. R. Castro, *Bioresour. Technol.* **2013**, 145, 280–284.

[132] S. Sahin, I. Ozmen, *J. Pharm. Biomed. Anal.* **2020**, 184, 113195.

[133] M. Bilal, M. Asgher, *Chem. Cent. J.* **2015**, 9, 1–14.

[134] M. Szcz-Antczak, T. Antczak, S. Bielecki, *Enzyme Microb. Technol.* **2004**, 34, 168–176.

[135] A. B. Moreira, V. H. Perez, G. M. Zanin, H. F. de Castro, *Energy Fuels* **2007**, 21, 3689–3694.

[136] M. H. El-Naas, S. A. Al-Muhtaseb, S. Makhlouf, *J. Hazard. Mater.* **2009**, 164, 720–725.

[137] G. b. Shan, J. m. Xing, M. f. Luo, H. z. Liu, J. y. Chen, *Biotechnol. Lett.* **2003**, 25, 1977–1981.

[138] J. Liao, H. Huang, *Int. J. Biol. Macromol.* **2019**, 138, 462–472.

[139] T. Petroviá, K. Markošová, Z. Hegyi, I. Smonou, M. Rosenberg, M. Rebroš, *Catalysts* **2018**, 8, 168.

[140] K. C. Badgujar, K. P. Dhake, B. M. Bhanage, *Process Biochem.* **2013**, 48, 1335–1347.

[141] H. Zhang, X. Fei, J. Tian, Y. Li, H. Zhi, K. Wang, L. Xu, Y. Wang, *Catal. Commun.* **2018**, 116, 5–9.

[142] A. M. Gañán-Calvo, J. M. López-Herrera, M. A. Herrada, A. Ramos, J. M. Montanero, *J. Aerosol Sci.***2018**, 125, 32–56.

[143] M.D. Hanwell, D.E. Curtis, D.C. Lonie, T. Vandermeersch, E. Zurek, G.R. Hutchison, *J. Cheminform.***2012**, 4, 17.

[144] J. Eberhardt, D. Santos-Martins, A.F. Tillack, S. Forli, *J. Chem. Inf. Model.* **2021**, 61, 3891–3898.

[145] S. Rosignoli, A. Paiardini, *Bioinformatics* **2022**, 38, 4233–4234.

[146] *The PyMOL Molecular Graphics System*, Version 2.0, Schrödinger, LLC.

[147] *Plane.py script*. Available from: https://github.com/Pymol-Scripts/Pymol-script-repo/blob/master/plane.py (Accessed on 2024.01.13).

[148] *R Core Team*. R: A language and environment for statistical computing. R Foundation for Statistical Computing, Vienna, Austria, **2022**. Available from: https://www.R-project.org/.

[149] *JASP Team*. JASP (Version 0.18.3) [Computer software], **2024**. Available from: https://jasp-stats.org/.

[150] G. K. Sharma, N. R. James, in *Recent Developments in Nanofibers Research*, IntechOpen, **2022**.

[151] G. Mitchell, Ed. , *Electrospinning: Principles, Practice and Possibilities*, Royal Society Of Chemistry, Cambridge, UK, **2015**.

[152] F. Liu, T. Nishikawa, S. Amiya, Q.-Q. Ni, Y. Murakami, *Sen-i Gakkaishi* **2012**, *68*, 49–54.

[153] Y. Dan, S. Chen, Y. Zhang, F. Xiang, *J. Polym. Sci. B Polym. Phys.* **2000**, *38*, 1069–1077.

[154] U. W. Gedde, M. S. Hedenqvist, *Fundamental Polymer Science*, Springer International Publishing, Cham, **2019**.

[155] M. Mathieu-Gaedke, A. Böker, U. Glebe, *Macro Chemistry & Physics* **2023**, *224*, 2200353.

[156] D. Russo, A. De Angelis, Christopher. J. Garvey, F. R. Wurm, M.-S. Appavou, S. Prevost, *Biomacromolecules* **2019**, *20*, 1944–1955.

[157] A. Van Loey, B. Verachtert, M. Hendrickx, *Trends in Food Science & Technology* **2001**, *12*, 94–102.

[158] Y. Wang, Y.-L. Hsieh, *Journal of Membrane Science* **2008**, *309*, 73–81.

[159] A. Al-Abduljabbar, I. Farooq, *Polymers* **2022**, *15*, 65.

[160] P. Castejón, K. Habibi, A. Saffar, A. Ajji, A. B. Martínez, D. Arencón, *Polymers***2018**, *10*, 33.

[161] D. N. Tran, K. J. Balkus, *Top Catal* **2012**, *55*, 1057–1069.

[162] A. C. Koch-Schmidt, K. Mosbach, *Biochemistry* **1977**, *16*, 2101–2105.

[163] D. Weiser, P.L. Sóti, G. Bánóczi, V. Bódai, B. Kiss, Á. Gellért, Z.K. Nagy, B. Koczka, A. Szilágyi, G. Marosi, L. Poppe, *Tetrahedron* **2016**, 72, 7335–7342.

[164] L.M.D.S. Brandão, M.S. Barbosa, R.L. Souza, M.M. Pereira, Á.S. Lima, C.M.F. Soares, *Biotechnol. Prog.* **2021**, 37, e3064.

[165] D.A. Sánchez, R.C. Alnoch, G.M. Tonetto, N. Krieger, M.L. Ferreira, *J. Biotechnol.* **2021**, 342, 13–27.

[166] Z. Yang, *Catalysts* **2019**, 9, 914.

[167] G. Hellner, Z. Boros, A. Tomin, L. Poppe, *Adv. Synth. Catal.* **2011**, 353, 2481–2491.

[168] D. Weiser, F. Nagy, G. Bánóczi, M. Oláh, A. Farkas, K. Szilágyi, Á. Gellért, G. Marosi, S. Kemény, L. Poppe, *Green Chem.* **2017**, 19, 3927–3937.